Free Radical Biology and Medicine 227 (2025) 521–535

Contents lists available at ScienceDirect

Free Radical Biology and Medicine

journal homepage: www.elsevier.com/locate/freeradbiomed

Distinct roles of ascorbic acid in extracellular vesicles and free form: Implications for metabolism and oxidative stress in presymptomatic Huntington's disease

Felipe A. Beltrán [a,b], Leandro Torres-Díaz L. [a,b,n], Paulina Troncoso-Escudero [a,b], Juan Villalobos-González [a,b], Gonzalo Mayorga-Weber [a,b], Marcelo Lara [c,q], Adriana Covarrubias-Pinto [a,b,d], Sharin Valdivia [a,b,p], Isidora Vicencio [a,b], Eduardo Papic [a,b], Carolina Paredes-Martínez [a,b], Mara E. Silva-Januário [e], Alejandro Rojas [b,f], Luis L.P. daSilva [e], Felipe Court [g,h,i], Abraham Rosas-Arellano [j], Luis Federico Bátiz [k,o], Patricio Rojas [c], Francisco J. Rivera [l,*], Maite A. Castro [a,b,m,**]

[a] Instituto de Bioquímica y Microbiología, UACh, Valdivia, Chile
[b] Center for Interdisciplinary Studies on Nervous System (CISNe), UACh, Valdivia, Chile
[c] Departamento de Biología, Universidad de Santiago de Chile, Santiago, Chile
[d] Institute of Biochemistry II, Goethe University School of Medicine, Theodor-Stern-Kai 7, 60590, Frankfurt am Main, Germany
[e] Faculdade de Medicina de Ribeirão Preto, Universidade de São Paulo, Ribeirão Preto, Brazil
[f] Instituto de Medicina, UACh, Valdivia, Chile
[g] Center for Aging Research and Healthy Longevity, Faculty of Sciences, Universidad Mayor, Santiago, Chile
[h] Geroscience Center for Brain Health and Metabolism (GERO), Santiago, Chile
[i] Buck Institute for Research on Aging, Novato, CA, USA
[j] Unidad de Imagenología, Instituto de Fisiología Celular, UNAM, CDMX, Mexico
[k] Centro de Investigación e Innovación Biomédica (CIIB), Universidad de Los Andes, Santiago, Chile
[l] Translational Regenerative Neurobiology Group (TReN), Molecular and Integrative Biosciences Research Program (MIBS), Faculty of Biological and Environmental Sciences, University of Helsinki, Helsinki, Finland
[m] Janelia Research Campus HHMI, Ashburn, VA, USA
[n] Departamento de Ciencias y Geografía, Facultad de Ciencias Naturales y Exactas, Universidad de Playa Ancha, Valparaíso, Chile
[o] Escuela de Medicina, Facultad de Medicina, Universidad de los Andes, Santiago, Chile
[p] Department of Biological and Chemical Sciences, Faculty of Medicine and Sciences, San Sebastián University, Tres Pascualas Campus, Concepción, Chile
[q] Escuela de Química y Farmacia, Facultad de Medicina y Ciencia, Universidad San Sebastián, Campus las Tres Pascualas, Concepción, Chile

ARTICLE INFO

Keywords:
Ascorbic acid
Exosomes
Glucose
Lactate
Neurodegeneration

ABSTRACT

Huntington's disease (HD) is a neurodegenerative disorder caused by a CAG trinucleotide repeat expansion in the first exon of the huntingtin gene. The huntingtin protein (Htt) is ubiquitously expressed and localized in several organelles, including endosomes, where it plays an essential role in intracellular trafficking. Presymptomatic HD is associated with a failure in energy metabolism and oxidative stress. Ascorbic acid is a potent antioxidant that plays a key role in modulating neuronal metabolism and is highly concentrated in the brain. During synaptic activity, neurons take up ascorbic acid released by glial cells; however, this process is disrupted in HD. In this study, we aim to elucidate the molecular and cellular mechanisms underlying this dysfunction. Using an electrophysiological approach in presymptomatic YAC128 HD slices, we observed decreased ascorbic acid flux from astrocytes to neurons, which altered neuronal metabolic substrate preferences. Ascorbic acid efflux and recycling were also decreased in cultured astrocytes from YAC128 HD mice. We confirmed our findings using GFAP-HD160Q, an HD mice model expressing mutant N-terminal Htt mainly in astrocytes. For the first time, we demonstrated that ascorbic acid is released from astrocytes via extracellular vesicles (EVs). Decreased number of particles and exosomal markers were observed in EV fractions from cultured YAC128 HD astrocytes and Htt-KD

* Corresponding author. Translational Regenerative Neurobiology Group (TReN), Molecular and Integrative Biosciences Research Program (MIBS), Faculty of Biological and Environmental Sciences, University of Helsinki, FI-00790 Helsinki, Finland
** Corresponding author. Instituto de Bioquímica y Microbiología, Facultad de Ciencias, Universidad Austral de Chile, casilla 547, Valdivia 5090000, Chile.
E-mail addresses: francisco.rivera@helsinki.fi (F.J. Rivera), macastro@uach.cl (M.A. Castro).

https://doi.org/10.1016/j.freeradbiomed.2024.12.001
Received 23 October 2024; Received in revised form 18 November 2024; Accepted 2 December 2024
Available online 9 December 2024

cells. We observed reduced number of multivesicular bodies (MVBs) in YAC128 HD striatum via electron microscopy, suggesting mutant Htt alters MVB biogenesis. EVs containing ascorbic acid effectively reduced reactive oxygen species, whereas “free” ascorbic acid played a role in modulating neuronal metabolic substrate preferences. These findings suggest that the early redox imbalance observed in HD arises from a reduced release of ascorbic acid-containing EVs by astrocytes. Meanwhile, a decrease in "free" ascorbic acid likely contributes to presymptomatic metabolic impairment.

1. Introduction

Huntington’s disease (HD) is a progressive, autosomal dominant neurodegenerative disorder that affects individuals of all ages and develops over 15–20 years. Motor dysfunction and cognitive abnormalities are common symptoms [1]. The disease is caused by an expanded CAG trinucleotide repeat in the Huntingtin gene [2] which causes major cell loss in the striatum, a basal ganglia region that integrates cortical information for behavioral output [3]. HD is characterized by widespread neurodegeneration with preferential deterioration of medium-sized spiny neurons (MSNs) in the striatum [3]. The major excitatory input to MSNs comes from the cortex (corticostriatal pathway) and the thalamus. The huntingtin gene encodes Huntingtin protein (Htt), which is essential for embryogenesis, is ubiquitously expressed in the adult nervous system [3], and is associated with all major organelles, including nuclei, endoplasmic reticulum (ER), Golgi complexes, microtubules, endosomal compartments [4–7]. Htt participates as key component regulating intracellular trafficking of vesicles, membrane proteins and organelles [8]. Glutamine expansions more than 40 repeats long within the Htt protein confers genetically dominant neurotoxicity and impair normal Htt function [9].

The brain makes up 2 % of total body mass in adult humans; however, it is responsible for 25 % of the total (resting) corporal energy consumption [10]. Deterioration of brain energy metabolism drives pathology in HD. Previous studies have shown that HD patients have markedly reduced glucose metabolism and transport [11–13]. Additionally, HD-associated metabolic dysfunction is accompanied by increased levels of reactive oxygens species and oxidative damage [14,15]. Furthermore, superoxide dismutase activity is impaired, and ascorbic acid levels are decreased in HD [16,17]. We have already published several studies on the function of ascorbic acid in neuronal metabolism [18–20]. Ascorbic acid, the reduced form of vitamin C, modulates neuronal metabolism between resting states and active periods (ascorbic acid metabolic switch) [18]. During synaptic activity, ascorbic acid is released into the extracellular space [21] and is taken up by neuronal cells [22]. Intracellular ascorbic acid inhibits glucose transport and stimulates lactate consumption in neurons [19,20]. We demonstrated that the ascorbic acid metabolic switch is impaired in HD [23,24], and that ascorbic acid flux from astrocytes to neurons is reduced in HD mice, disrupting proper metabolic modulation and compromising the redox balance in neurons [24].

Astrocytes recycle vitamin C in the brain [25], and during synaptic activity, glutamate stimulates ascorbic acid release from intracellular reservoirs [21,26]. However, the molecular basis of ascorbic acid efflux is not well understood. Ascorbic acid is oxidized within the neurons alongside other oxidative species generated during synaptic activity. Oxidized ascorbic acid (dehydroascorbic acid) can be released through glucose transporters (GLUTs), GLUT1 or GLUT3 [27], and astrocytes can take it up through GLUT1 [28,29]. Astrocytes contain high concentrations of glutathione, express high levels of dehydroascorbic acid reductases [28], maintain redox homeostasis, and maintain an adequate supply of metabolic substrates to neurons during synaptic activity.

In summary, Htt plays a key role in regulating intracellular trafficking, a function that is lost when Htt is mutated, as seen in HD. Ascorbic acid is essential for regulating neuronal metabolism and maintaining redox balance, both of which are disrupted in HD. Since ascorbic acid flux from astrocytes to neurons is impaired in presymptomatic HD, we hypothesized that the release of ascorbic acid from astrocytes involves a mechanism related to Htt’s role in intracellular trafficking. Building on this idea, here, we show for the first time, to our knowledge, that ascorbic acid can be released from astrocytes via extracellular vesicles (EVs). We also demonstrate that impaired release of astrocytic ascorbic acid via EVs contributes to oxidative stress in HD, while the presence of "free" ascorbic acid is associated with early metabolic dysfunction in the disease. To demonstrate this, we investigated the role of ascorbic acid in modulating neuronal metabolism using acute brain slices, as we had done previously [24]. For this, we used YAC128 HD mice, a widely utilized model that expresses the full-length mutant Htt protein and is well-suited for studying the presymptomatic stages of HD. To investigate the astrocytic contribution of mutant Htt to ascorbic acid flux impairment in HD, we employed GFAP-HD160Q mice, which express the mutant N-terminal Htt specifically in astrocytes [30]. We found ascorbic acid flux from astrocytes to neurons was reduced in acute slices from both presymptomatic mice models. We also found ascorbic acid efflux and recycling were decreased in cultured astrocytes from YAC128 mice. Cultured HD-astrocytes and KD-Htt cells secreted fewer EVs and less ascorbic acid, and we detected reduced multivesicular bodies (MVBs) in the striatal HD via electron microscopy (EM). Using neuronal cultures exposed to EVs containing ascorbic acid and "free" ascorbic acid, we demonstrated that the former could reduce ROS, while the latter modulates glucose and lactate transport. Therefore, our results suggest impaired MVB biogenesis decreases EV-mediated ascorbic secretion from astrocytes in HD, promoting early oxidative stress, while early metabolic failure would be related to “free” ascorbic acid.

2. Results

2.1. Glial-neuron ascorbic acid flux is impaired in presymptomatic YAC128 mice

Ascorbic acid flux from astrocytes to neurons during synaptic activity protects neurons against oxidative damage, modulates neuronal metabolism and facilitates optimal ATP production. Previous studies have shown that glial-neuron ascorbic acid flux is impaired in R6/2 mice [24], which express exon 1 of human Htt protein containing 150 CAG repeats. These mice exhibit rapid disease progression are often used to model juvenile-onset HD, with symptoms manifesting as early as one month of age [31]. While this model has been valuable for certain types of research, its rapid and severe phenotype does not accurately reflect the gradual progression of HD observed in humans, particularly in the adult-onset form. YAC128 mice express the entire human HD gene containing 128 CAG repeats, develop motor abnormalities starting at 4–6 months old and exhibit age-dependent striatal atrophy as well as striatal neuronal loss [32–34]. This model exhibit an adult onset of symptoms and a more progressive disease course, being particularly useful for studying the presymptomatic stages of the disease, which are critical for understanding the early pathophysiological changes that precede overt symptoms. The ability to investigate presymptomatic issues is of significant clinical value, as it supports the development of early intervention strategies. Using YAC128 corticostriatal acute slices we found that glucose cannot sustain field excitatory postsynaptic potentials (fEPSPs) when neuronal intracellular concentrations of ascorbic acid are high (Fig. 1). We evoked fEPSPs by stimulating the corticostriatal pathway (Fig. 1A) and investigated how changes in glucose

affected synaptic activity. Synaptic responses in WT and presymptomatic YAC128 mice recovered quickly following glucose deprivation when we reapplied it (Fig. 1B) (92.4 ± 1.89 %; control, Fig. 1C, left). Glucose also restored fEPSPs in presymptomatic YAC128 mice (87.37 ± 6.57 %; control; Fig. 1C). In the presence of 100 μM alpha-cyano-4-hydroxycinnamic acid (4-CIN), which inhibits neuronal monocarboxylate (lactate) transporter MCT2 [35] recovery was not observed in WT mice (19,61 ± 0.91 %; 4-CIN, Fig. 1C); however, the ability of glucose to sustain fEPSPs in YAC128 mice was unaffected (85, 58 ± 4,41 %; 4-CIN, Fig. 1C). These results strongly suggest that the ANLS (astrocyte-neuron lactate shuttle) is necessary to maintain adequate ATP levels in cells within the corticostriatal circuit and is impaired HD neurons. We applied extracellular ascorbic acid to presymptomatic YAC128 slices and observed a strong decrease in fEPSP amplitude following glucose deprivation (19.33 ± 3.28 %; 4-CIN + AA, Fig. 1C), suggesting that exogenous extracellular ascorbic acid concentrations facilitate ANLS function in these slices. We performed paired-pulse facilitation (PPF) experiments to account for presynaptic alterations (Fig. 1D, E, F, G and H). Neural facilitation, also known as PPF, is caused by increased Ca^{2+} mediated release of neurotransmitter-containing synaptic vesicles. We did not observe any differences in neural facilitation in YAC128 mice compared to WT controls suggesting presynaptic terminals were not altered (Fig. 1F, G and H). In conclusion, the ANLS and the ascorbic acid metabolic switch are impaired in the striatum of presymptomatic YAC128 mice because their glial cells release less ascorbic acid.

We analyzed mRNA transcript levels of nutrient transporters associated with the ANLS and ascorbic acid metabolic switch in the striatum (Fig. 2) and found YAC128 mice had increased expression of neuronal MCT2 [35] (lactate uptake, Fig. 2B) and astrocytic MCT4 [36] (lactate release, Fig. 2C), but not MCT1 [37] (Fig. 2A), suggesting increased lactate flux from astrocytes to neurons (Fig. 2B and C). However, we also found that synaptic activity in presymptomatic HD neurons is not lactate-dependent (Fig. 1C); therefore, changes in MCT2/4 expression could be part of a compensatory mechanism. We observed an increase in GLUT1 expression in presymptomatic YAC128 samples (Fig. 2D). GLUT1 is ubiquitously expressed in the brain and at high levels in glial and endothelial cells of the blood-brain barrier (BBB) [38]. GLUT1 is poorly expressed in neurons, and YAC128 mice have decreased GLUT3 expression [39] (neuronal transporter, Fig. 2E). Therefore, it is unlikely that neuronal GLUT1 overexpression under pathological conditions explains the "lactate-independent" behavior we observed in our electrophysiological experiments. Indeed, decreased GLUT3 expression could be a compensatory response to an impaired ANLS. Finally, we did not observe any changes in the mRNA levels of the neuronal ascorbic acid transporter, SVCT2 (Fig. 2F) [22].

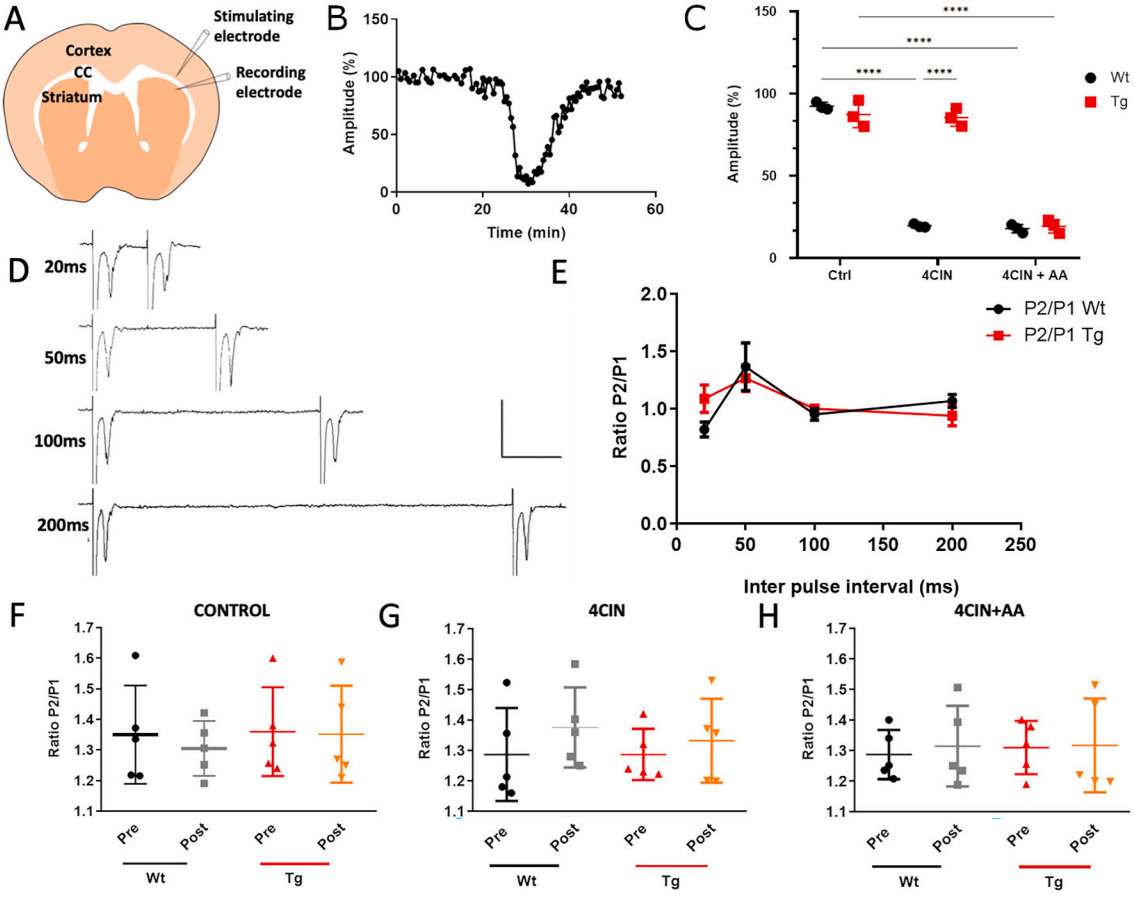

Fig. 1. Glia-Neuron ascorbic acid flux is impaired in YAC 128 mice. A. Schematic drawing of our experimental set-up shows the stimulating electrode in the corpus callosum (CC) and the recording electrode in the dorsolateral striatum. **B.** Time course of fEPSC amplitudes in control experiments (with and without glucose). **C.** Individual values plot represent fEPSC amplitudes (%) after glucose deprivation (amplitude recovery after 50 min) with 4CIN (alpha-cyano-4-hydroxycinnamic acid) and 4CIN + ascorbic acid (AA) in presymptomatic mice. **D.** Representative fEPSCs evoked at 20, 50, 100 and 200 ms intervals between pulses in control (WT) mouse slices. Facilitation occurs at 50 ms. Calibration Bar: 100 pA, 5 ms. **E.** Paired pulse ratios (P2/P1) of inter-pulse intervals described in (D) before electrophysiology experiments for YAC128 (red) and control (WT) (black) mouse slices. **F.** PPR at 50 ms pulse interval in YAC128 and control (WT) mouse slices before (Pre) and after (Post) electrophysiology during glucose deprivation experiments. **G.** PPR described in F in glucose-deprived conditions + 4-CIN. **H.** PPR described in F in glucose-deprived conditions + 4-CIN + AA. Two-way ANOVA with multiple comparisons, n = 5 (B, C) ****$p < 0.0001$. One-way ANOVA followed of Tukey test, n = 5 (D–H). (For interpretation of the references to colour in this figure legend, the reader is referred to the Web version of this article.)

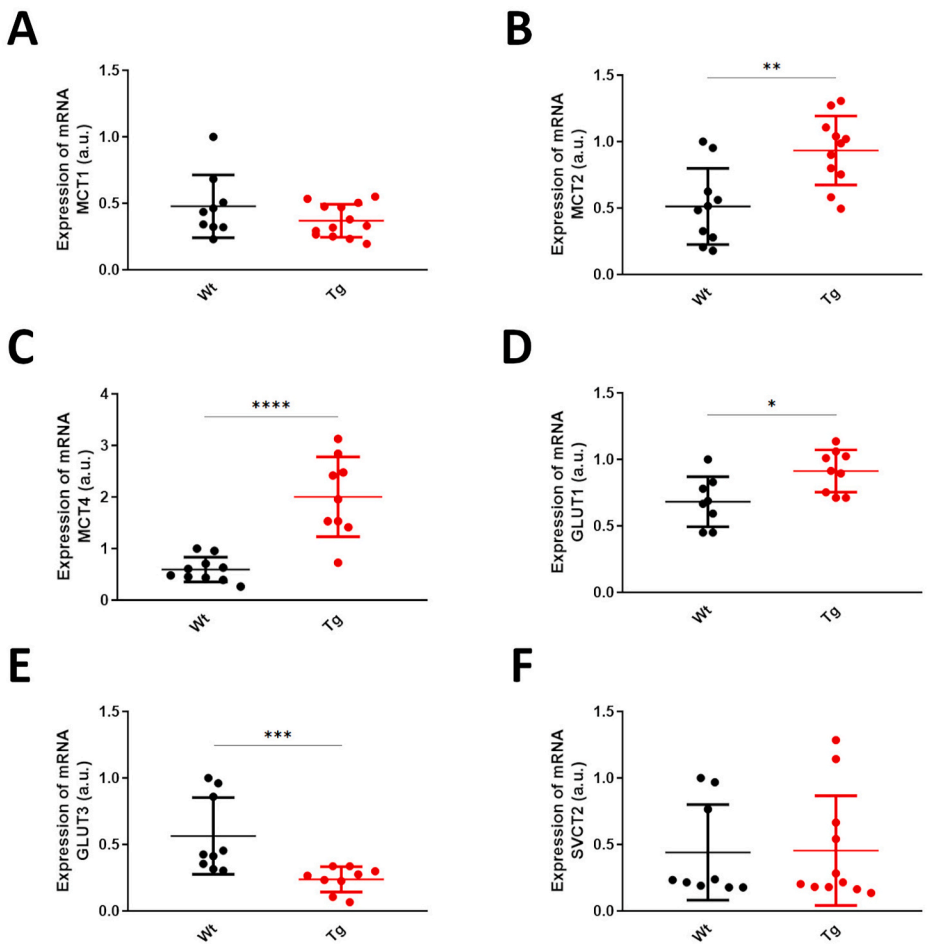

Fig. 2. mRNA levels of nutrient transporters associated with ANLS and the ascorbic acid metabolic switch in YAC128 mice. A. Monocarboxylate transporter MCT1, **B.** MCT2 and **C.** MCT4 mRNA expression levels in control (WT) (black) and YAC128 (Tg) (red) striatum. **D.** Glucose transporter GLUT1 and **E.** GLUT 3 mRNA expression levels in control (WT) (black) and YAC128 (Tg) (red) striatum. **F.** Ascorbic acid transporter SVCT2 expression levels in control (WT) (black) and YAC128 (Tg) (red) striatum. Student's t-test, n = 6 for every condition, $*p < 0.05$, $**p < 0.01$, $***p < 0.001$, $****p < 0.0001$. (For interpretation of the references to colour in this figure legend, the reader is referred to the Web version of this article.)

2.2. Ascorbic acid release from astrocytes is decreased in HD

Astrocytes recycle ascorbic acid by reducing dehydroascorbic acid (DHA) produced during synaptic activity. We investigated the capacity of striatal cultured astrocytes to recycle DHA to ascorbic acid (Fig. 3A and B). We generated DHA via ascorbate oxidase-mediated ascorbic acid oxidation [40], incubated astrocytes in DHA-containing media and stimulated ascorbic acid recycling using L-glutamate. We determined ascorbic acid content via HPLC but did not observe any significant changes in ascorbic acid recycling or GSH/GSSG content in WT or YAC128 astrocytes (Fig. 3B and C). DHA reduction is catalyzed by GSH-dependent enzymes such as thioredoxin reductase (TrxR1) and glutaredoxin 1 (Grx1). We did observe decreased glutamate-stimulated ascorbic acid release from YAC128 astrocytes (Fig. 3D and E), suggesting while ascorbic acid recycling in astrocytes may not be affected in HD, glutamate-stimulated ascorbic acid release from astrocytes is impaired.

We performed electrophysiological recordings in brain acute slices derived from GFAP-HD160Q mice (Fig. 4) to test whether impaired astrocytic ascorbic acid release is responsible for early metabolic failure in HD. GFAP-HD160Q mice express the N-terminal of human Htt containing 160 repeats for polyglutamine under the glial fibrillar acidic protein (GFAP) promoter [30]. The expression of mutant huntingtin in astrocytes of the GFAP-HD160Q mouse brain leads to age-dependent HD symptoms, with motor disabilities beginning at 12 months of age [29]. As in YAC128 mice, glucose re-application after glucose deprivation produced a fast recovery of synaptic responses in acute slices from presymptomatic GFAP-HD160Q mice (Fig. 4A, B and C), and glucose was able to restore fEPSPs when we inhibited neuronal MCT2 (100 μM 4-CIN) in these mice (74.48 ± 2.62 %; 4-CIN; Fig. 4C, center). Extracellular ascorbic acid also abolished glucose-mediated restoration of fEPSPs in the presence of 4CIN (28.894 ± 3.16 %, 4CIN + AA; Fig. 4C, right) in these mice. We tested nutrient transporter expression in the striatum of GFAP-HD160Q via RT-qPCR (Fig. 5) and found a slight increase in MCT1 expression (Fig. 5A), however, we did not observe any changes in MCT2, MCT4, GLUT1, GLUT3 or SVCT2 expression (Fig. 5 B, C, D, E and F), suggesting the compensatory mechanisms we proposed for YAC128 mice are not induced by impaired release of ascorbic acid from astrocytes. Therefore, expression of mHtt in astrocytes, which impairs ascorbic acid release from these cells, seems to be responsible for early metabolic and redox imbalance in HD.

2.3. Extracellular vesicles secreted from astrocytes contain ascorbic acid

The molecular mechanism underlying ascorbic acid release from cells is not well known. It has been proposed that ascorbic acid could be released via several mechanisms, including glutamate/ascorbate heteroexchange [41], volume-sensitive organic anion channels [42,43], exocytosis [42], hemichannels [44], or the ascorbic acid transporter SVCT2 [45], but this is still debated. Extracellular vesicles (EVs)

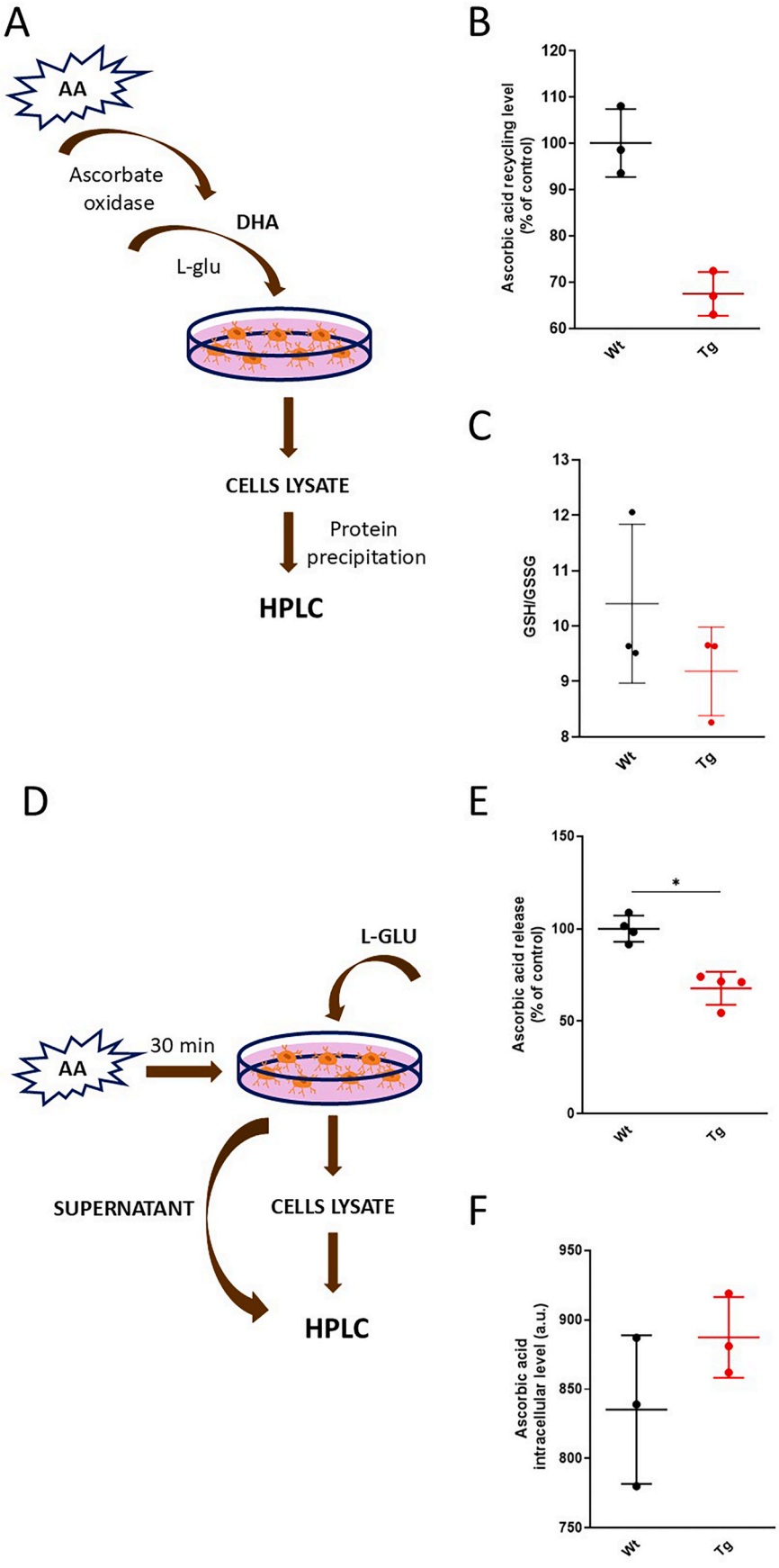

(caption on next page)

Fig. 3. Ascorbic acid efflux and recycling are impaired in YAC128 mouse primary astrocytes. A. Schematic representation of DHA incubation experiment investigating ascorbic acid (AA) recycling via HPLC. YAC128 and control primary striatal astrocyte cultures were incubated with DHA, then L-glu was added as described in methods. Cells were lysed for AA detection by HPLC. **B.** AA recycling levels in YAC128 (Tg) and control (WT) primary striatal astrocytes. **C.** Intracellular GSH/GSSG content in YAC128 (Tg) and control (WT) primary striatal astrocytes. **D.** Schematic representation of AA incubation experiment with primary striatal astrocytes. YAC128 and control primary striatal astrocytes were incubated with AA for 30 min, then L-glu was added as described in methods. Cells were lysed, and the cell growth medium (supernatant) was collected to detect AA via HPLC. **E.** AA efflux in YAC128 (Tg) and control (WT) primary astrocytes. **F.** AA compartmentalization (intracellular level) in YAC128 (Tg) and control (WT) primary astrocytes. Student's t-test, n = 3 for every condition, $*p < 0.05$.

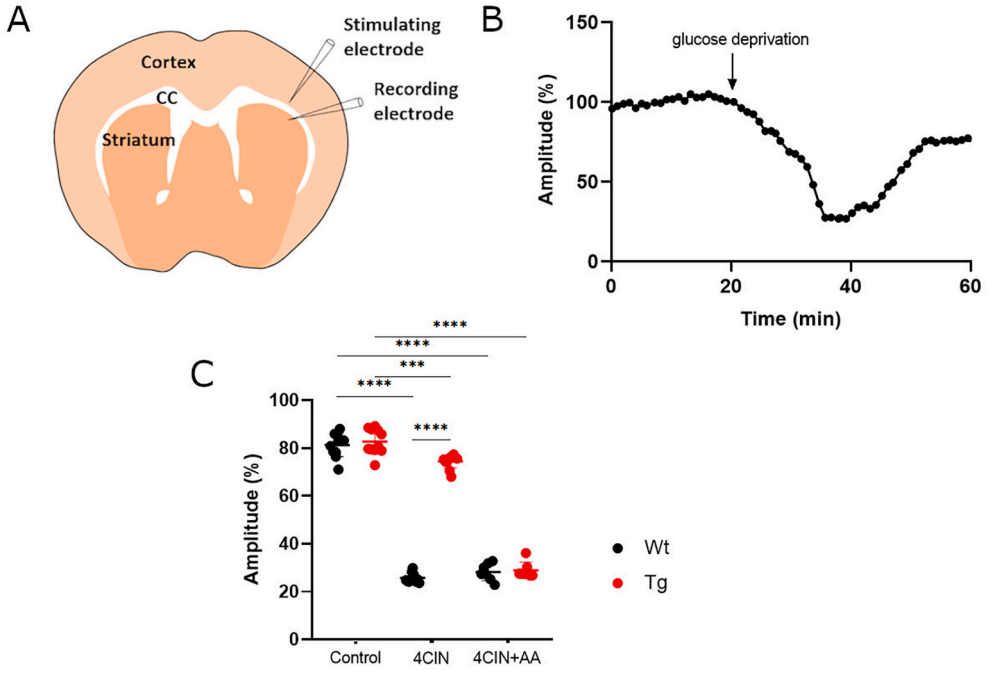

Fig. 4. Glia-Neuron ascorbic acid flux is impaired in GFAP-HD160Q mice. A. Schematic drawing of the experimental set-up showing positions of the stimulating electrode in the corpus callosum (CC) and the recording electrode in the dorsolateral striatum in mouse brain slices. **B.** Time course of fEPSC amplitudes in control experiments. **C.** Individual values plot represent fEPSC amplitudes (%) after glucose deprivation (amplitude recovery after 55 min) with 4CIN (alfa-cyano-4-hydroxycinnamic acid) and 4CIN + ascorbic acid (AA) in presymptomatic mice. One-way ANOVA followed by the Tukey post-test, n = 11 (CTRL and 4CIN), n = 7 (4CIN + AA, WT), n = 7 (4CIN + Asc, TG), $***p < 0.001$, $****p < 0.0001$.

facilitate intercellular communication in many cellular processes [46], and Htt protein facilitates intracellular vesicular trafficking. We tested ascorbic secretion from astrocytes through EVs. We harvested EVs from primary astrocyte cultures and tested via Western blot for exosomal markers (Fig. 6A and B). We determined ascorbic acid content via HPLC (Fig. 6C, red arrow) demonstrating EV-mediated ascorbic acid secretion for the first time.

2.4. Astrocytic EV secretion is decreased in HD

Upon revealing that EVs contain ascorbic acid, we tested EV secretion from GFAP-HD160Q striatal astrocytes. We harvested EVs from WT and GFAP-HD160Q astrocytes cultures of equal cellular density and determined their exosomal cargo via Western blot for Alix and Tsg101 (Fig. 7B). A decreased detection of Alix and Tsg101 was observed in samples from GFAP-HD160Q astrocyte-derived EVs, suggesting these cells secreted fewer EVs. This idea was confirmed via scanning electron microscopy (SEM; Fig. 7C) and nanoparticle tracking analyses (NTA; Fig. 7D). We analyzed EV fractions via nanoparticle tracking analyses (NTA) and found GFAP-HD160Q astrocytes secreted fewer 115-185 nm-sized EVs (Figs. 7D) and 50 % fewer EVs in total, demonstrating that mHtt alters EV secretion. We then tested whether loss of Htt function alters EV secretion. Using CRISPR/Cas9 technology we generated a HEK293T cells partially ablated for Htt expression (Fig. 7E; HEK-KD-Htt). We conducted Western blots (Fig. 7F) and NTA (Fig. 7G, H and I) for exosomal cargoes and found that HEK-KD-Htt cells secreted fewer EVs, suggesting loss of Htt function decreases EV secretion from HD astrocytes.

We tested EV-mediated ascorbic acid release from YAC128 astrocytes (Fig. 8). We loaded primary cultures of striatal YAC128 astrocytes with ^{14}C-ascorbic acid and then harvested the EVs secreted (Fig. 8A, left). We normalized the ^{14}C-ascorbic acid content of the EVs to the total protein content of the cell lysate and found it was decreased in YAC128 samples (Fig. 8A, middle). However, when we normalized EV ^{14}C-ascorbic acid content to the total protein content of the EV fraction lysates, we did not observe any significant difference between YAC128 and WT samples (Fig. 8A, right). Therefore, we conclude EV secretion is decreased in HD cells, but ascorbic acid loading into EVs is not affected. We confirmed this conclusion via nanosight analyses, which showed decreased HD cells secreted for EVs greater than 100 nm in size (Fig. 8B, C, and D).

We also tested the ability of EVs containing ascorbic acid to maintain redox balance in primary cultures of striatal neurons obtained from YAC128 mice. EVs containing ascorbic acid obtained from WT astrocytes were able to reduce reactive oxygen species (ROS) in WT and YAC128 neurons (Fig. 8E), as well as 1 mM ascorbic acid directly. However, similar fractions of EVs (normalized by total protein content from the cell lysate of astrocytes) harvested from YAC128 astrocytes failed to decrease ROS in either WT or YAC128 neurons (Fig. 8E). This is consistent with our previous finding demonstrating that YAC128 astrocytes secrete fewer EVs containing ascorbic acid.

Finally, we tested if EVs containing ascorbic acid were able to inhibit glucose uptake in striatal neurons from mice (Fig. 8F). Ascorbic acid can

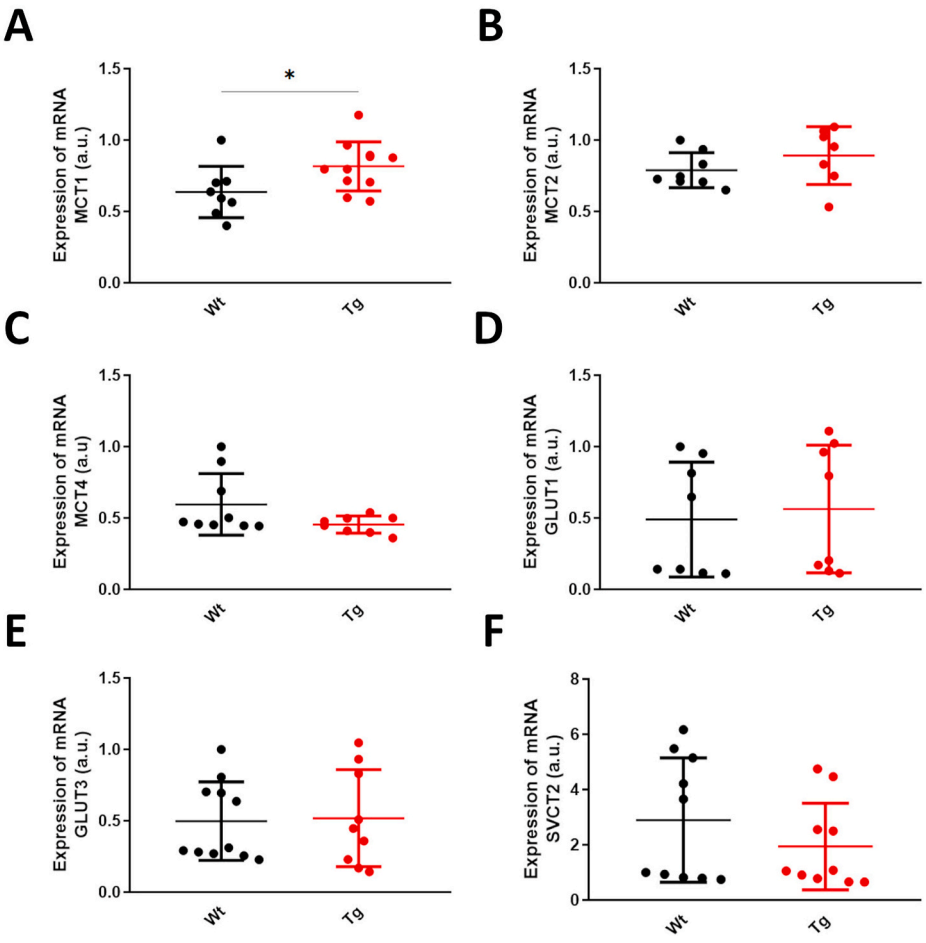

Fig. 5. mRNA levels of nutrient transporters associated with ANLS and the ascorbic acid metabolic switch in GFAP-HD160Q mice A. Monocarboxylate transporter MCT1, **B.** MCT2 and **C.** MCT4 mRNA expression in control (WT) (black) and GFAP-HD160Q (Tg) (red) striata. **D.** Glucose transporter GLUT1 and **E.** GLUT3 mRNA expression in control (WT) (black) and GFAP-HD160Q (Tg) (red) striatum. **F.** AA transporter SVCT2 expression in control (WT) (black) and GFAP-HD160Q (Tg) (red) striatum. Student's t-test, n = 7–11 for every condition, $*p < 0.05$. (For interpretation of the references to colour in this figure legend, the reader is referred to the Web version of this article.)

modify substrate preference in neurons by inhibiting glucose uptake and stimulating lactate transport [19,20,23,24], (Fig. 8F). Surprisingly, EVs containing ascorbic acid did not inhibit deoxyglucose (DOG) uptake in any case, suggesting that ascorbic acid secreted through EVs is used to maintain redox balance, while ascorbic acid secreted directly or "free" would be responsible for modulating metabolic substrate preference.

EVs are a heterogeneous population of exosomes and ectosomes. Exosomes are formed via the fusion of multivesicular bodies (MVBs), a type of late endosome containing intraluminal vesicles (IVs) [47], with the plasma membrane. In contrast, ectosomes are formed via plasma membrane shedding [48]. Htt has a central role in controlling intracellular trafficking [8]; therefore, we hypothesized that the impaired EV secretion we observed in HD cells could be caused by impaired MVB biogenesis. We performed transmission electron microscopy (TEM) in the striatum of YAC128 mice (Fig. 8G) to test our hypothesis. We quantified the number of MVB per area (Fig. 8H), MVB area (Fig. 8I), number of IVs per MVB (Fig. 8J) and IVs area (Fig. 8K) and observed fewer MVs per area in HD cells but did not observe any changes in the other parameters. Therefore, we conclude that loss of Htt function reduces MVB biogenesis and secretion of EVs containing ascorbic acid.

3. Discussion

HD is characterized by a failure in brain energy metabolism [13,14,49–51], even in its presymptomatic stages [11,24]. In the present study, we have shown alterations in neuronal substrate energetic preferences in brain slices from presymptomatic YAC128 mice. Although BACHD is the most widely studied animal model for HD, we chose to use YAC128 for this study. In BACHD, HD onset occurs at 2 months of age, meaning that studies conducted during the presymptomatic stages could be confounded by hormonal fluctuations associated with the onset of puberty, which typically occurs around 1 month of age. The YAC128 mouse is another widely studied full-length model of Huntington's disease (HD). These mice exhibit abnormal behavior starting at 4–6 months of age [34] and show degeneration in both the striatum and cortex [52]. R6/2 mice (used in our previous work [24]) exhibit a very aggressive form of HD and display overt behavioral symptoms as early as 4–5 weeks of age [53], and some authors argue that subtle abnormalities are present at 3 weeks of age. Our results in YAC128 mice confirm the idea that brain metabolism begins to fail before symptoms occur in HD. We have shown that changes in energetic substrate preferences are related to decreased ascorbic acid flux between astrocytes and neurons and impairment of the ascorbic acid metabolic switch [18]. The ascorbic acid metabolic switch describes astrocytic ascorbic acid release in response to glutamatergic activity, shifting neuronal energy substrate preference towards lactate and increasing their antioxidant capacity. Therefore, if neurons cannot obtain enough energetic substrates upon constant stimulation, they cannot exert synaptic responses. We did not observe any synaptic responses in 4CIN-treated WT slices, indicating the importance of monocarboxylates for sustained synaptic activity.

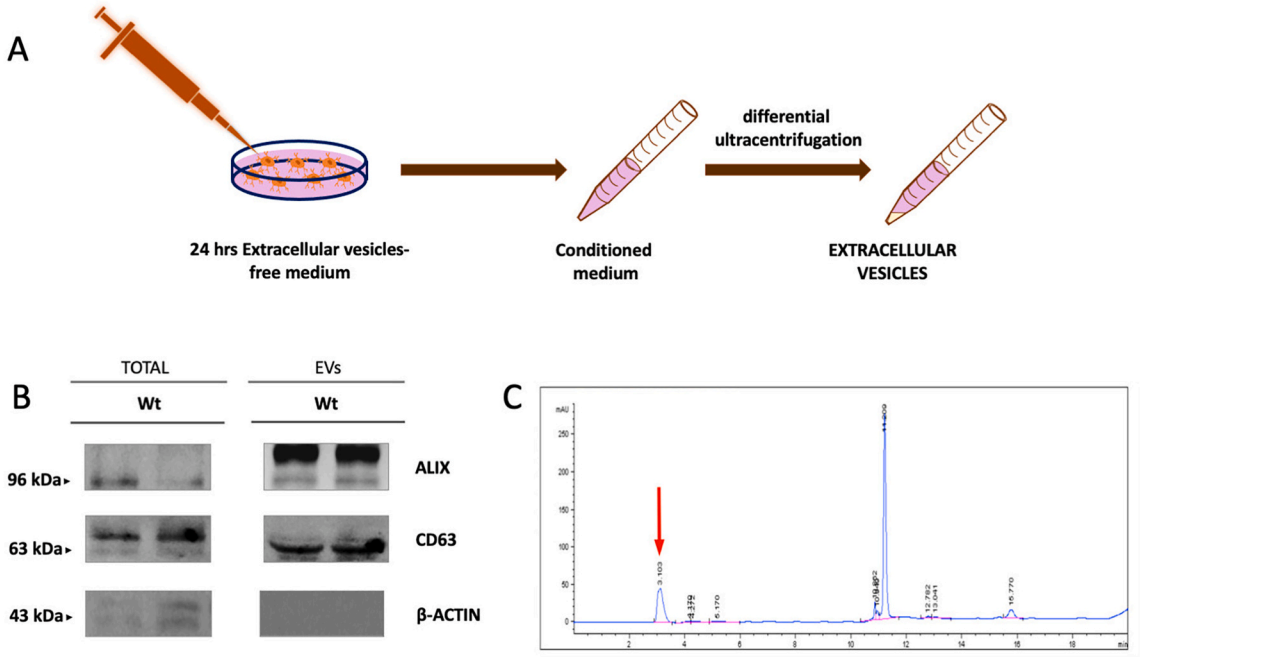

Fig. 6. Ascorbic acid is released through EVs from primary astrocytes. A. Schematic representation of EV harvesting from primary striatal astrocyte cultures. The primary astrocytes cell growth medium was replaced 24 h before harvesting with an EV-free medium. Exosomes were then harvested via differential centrifugation as described in the methods. **B.** Western blots for the exosomal markers Alix and CD-63 in EV enriched fractions obtained from WT primary astrocytes. **C.** Representative ascorbic acid (AA) HPLC detection (red arrow) in EV enriched fractions obtained from primary astrocytes. (For interpretation of the references to colour in this figure legend, the reader is referred to the Web version of this article.)

Conversely, HD slices exhibited promiscuous substrate preferences during sustained synaptic activity, decreasing striatal output and basal ganglia function. Exogenous ascorbic acid reversed this effect, indicating extracellular ascorbic acid does not increase during synaptic activity in presymptomatic YAC128 mice. These findings are consistent with those made by Dorner et al. [54], who reported altered ascorbic acid homeostasis in HD mice.

Astrocytes are the most abundant cells in the central nervous system and maintain the extracellular ascorbic acid concentration. Glutamate increases extracellular ascorbic acid concentration during glutamatergic synaptic activity [26,55–58]. It has been proposed that ascorbic acid could be released through several mechanisms, including glutamate/ascorbate heteroexchange [41], volume-sensitive organic anion channels [21,43], exocytosis [42] and hemichannels [44]. SVCT2-mediated intracellular ascorbic acid accumulation is driven by sodium gradients [59]; however, Portugal and colleagues [45] proposed that SVCT2 could drive ascorbic acid release. Their hypothesis was based on the observation that sulfinpyrazone (or lack of sodium) inhibits ascorbic acid efflux. However, sulfinpyrazone inhibits SVCTs non-specifically, and astrocytic SVCT2 expression has been discarded in vivo [60]. We have demonstrated that astrocytic ascorbic acid release occurs via extracellular vesicles for the first time. Previous studies have shown that exosomes have various roles in energy metabolism. Prostate exosomes can produce ATP from glycolysis [61], oligodendrocyte-to-neuron signaling through EVs enhances axonal mitochondria ATP production [62] and glycolytic enzymes are found in prostate exosomes in several species [63]. Finally, the products of amino acid, carbohydrate, purine, and vitamin B metabolism have all been detected in EVs [64]. On the other hand, the burst in energy metabolism and ATP production to maintain synaptic activity produces a significant ROS and oxidant species [65]. Our data indicate that ascorbic acid released through EVs is preferentially used to maintain redox balance. It has been shown that several soluble antioxidant enzymes are present in extracellular vesicles. Proteomic analyses have demonstrated the presence of superoxide dismutase, catalase, glutathione peroxidase, glutathione reductase, and other enzymes carried by extracellular vesicles [66,67]. Indeed, the antioxidant properties of extracellular vesicles have been shown to protect against seizure-induced neuronal damage [68]. Therefore, the release of "free" ascorbic acid (through the mechanisms discussed below) should play a key role in modulating energy substrate preferences in neurons, while ascorbic acid released through extracellular vesicles mainly acts as an antioxidant to control ROS and oxidant species produced during synaptic activity.

We found KD-Htt HEK cells secreted fewer EVs supporting the idea that EV secretion is Htt-dependent. Therefore, brain energy metabolism and redox imbalance failure in HD could be due to altered MVB biogenesis and EV secretion from astrocytes, consistent with work from Boussicault and colleagues [69]. They proposed that mutant astrocytes adversely affect neuronal metabolism in a non-cell-autonomous manner in BACHD (HD) mice. Htt protein is ubiquitously expressed; however, mutant Htt initially causes neuronal degeneration in the striatum, possibly because the striatum is highly energy-dependent and thus is a high producer of ROS and oxidant species. Indeed, the citric cycle inhibitor 3-Nitropropionic acid (which inhibits succinate dehydrogenase, a complex II enzyme) induces HD-like symptoms in mice [70].

The tertiary structure of Htt is consistent with its proposed role as a scaffold protein. It has several motifs that anchor it to membranes and an N-terminal signal sequence that reversibly associates with the ER, endosomes and autophagosomes [71]. Htt also has several interacting partners involved in vesicular and intracellular trafficking that facilitate interactions with the molecular motors kinesin, dynactin and myosin [72–77], and it interacts with Rab GTPases such as Rab 5 or Rab11 [72,77]. Wild-type Htt is incredibly important for proper intracellular transport of vesicles, organelles, and protein trafficking to the cell surface. All these findings are consistent with our data and highlight Htt participation in MVB biogenesis and exosome secretion. MVB biogenesis is regulated by the Hrs protein, which recruits ESCRT-I, II and III complexes required for the formation of intraluminal vesicles [78]. Reduced Hrs expression would reduce MVB formation and increase late endosome size [78]. Hrs also interacts with Huntingtin-associated protein-1

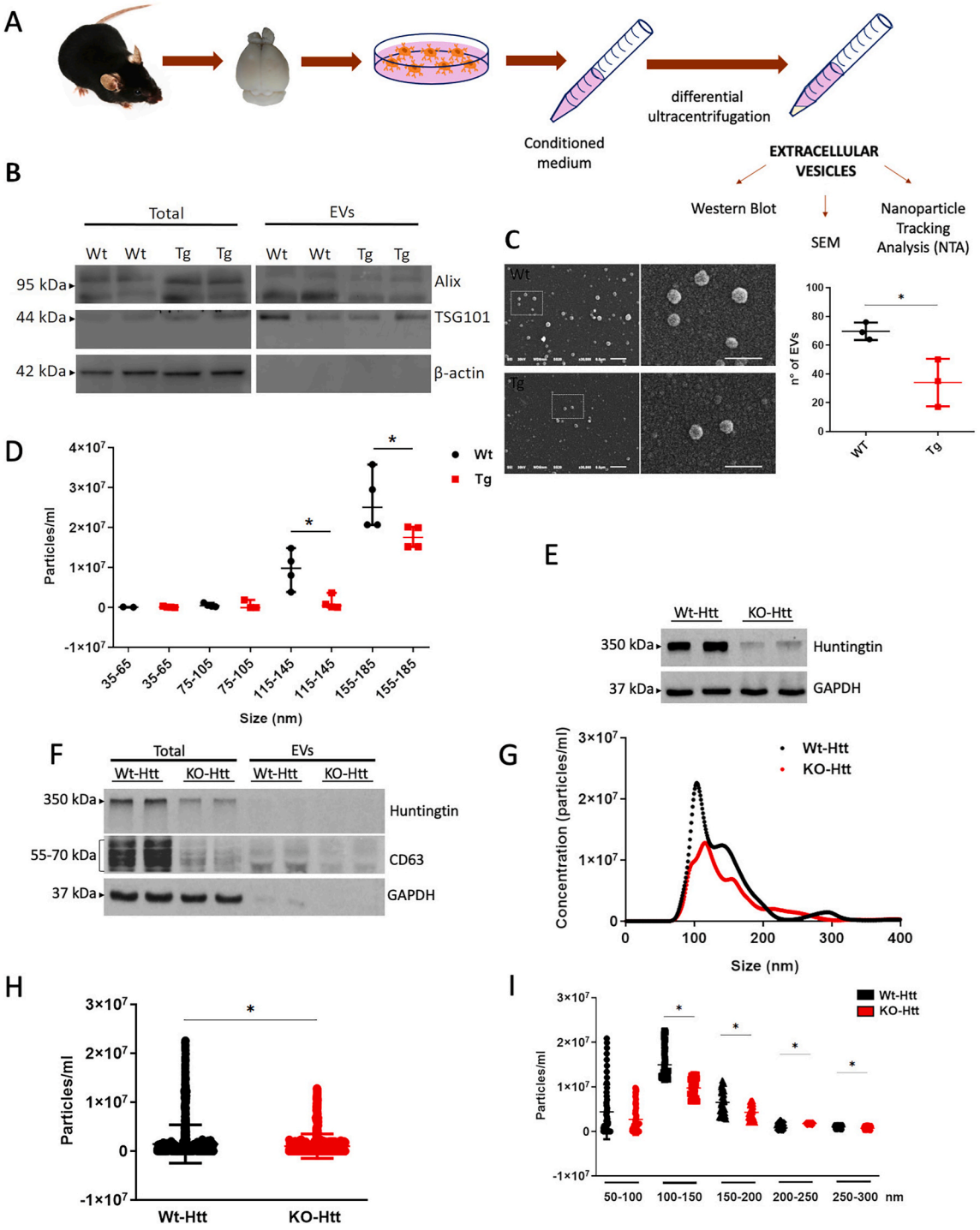

Fig. 7. EV secretion is dependent on Htt expression. A. Schematic representation of EV harvesting from YAC128 primary striatal astrocyte cultures. Total extract protein from harvested EVs and intact fractions of EVs were analyzed as follows. **B.** Western blots for the exosomal marker Alix in EV enriched fractions obtained from YAC128 primary astrocyte cultures. **C.** *Left:* Representative SEM images for EVs extracted from WT (top) and YAC128 (bottom) primary astrocyte cultures. *Right:* Total particles count per area from EVs obtained from WT and YAC128 primary astrocyte cultures. **D.** Total particle count per size interval obtained from nanoparticle tracking analyses. **E.** Western blots for Htt from HEK and HEK KD-Htt total protein extracts. **F.** Western blots for the exosomal marker CD63 and Htt in EV enriched fractions from HEK and HEK KD-Htt cultures. **G.** A histogram showing the distribution of HEK and HEK KD-Htt EV sizes. **H.** Total particle count from EVs obtained from HEK or HEK KD-Htt cell cultures. **I.** Total particle count per size interval obtained from nanoparticle tracking analyses. Student's t-test, n = 3 for every condition (C), $*p < 0.05$. One-way ANOVA followed by the Tukey post-test, n = 4 for every condition (D), $*p < 0.05$. Student's t-test, n = 4 for every condition (H), $*p < 0.05$. One-way ANOVA followed by the Tukey post-test, n = 4 for every condition (D), $*p < 0.05$.

(HAP1) via coiled-coil (spiral) junctions located between the central domains of both proteins in early endosomes.

We observed increased monocarboxylate transporter 2 (MCT2) (neuronal lactate uptake [35] and MCT4 expression in YAC128 mice (astrocytic lactate efflux [36]. Increased astrocytic-neuron lactate flux could be a compensatory mechanism. However, SVCT2 intracellular trafficking [24,79] and ascorbic acid metabolic switch [18] are impaired in HD neurons, which may be why YAC128 mice display this

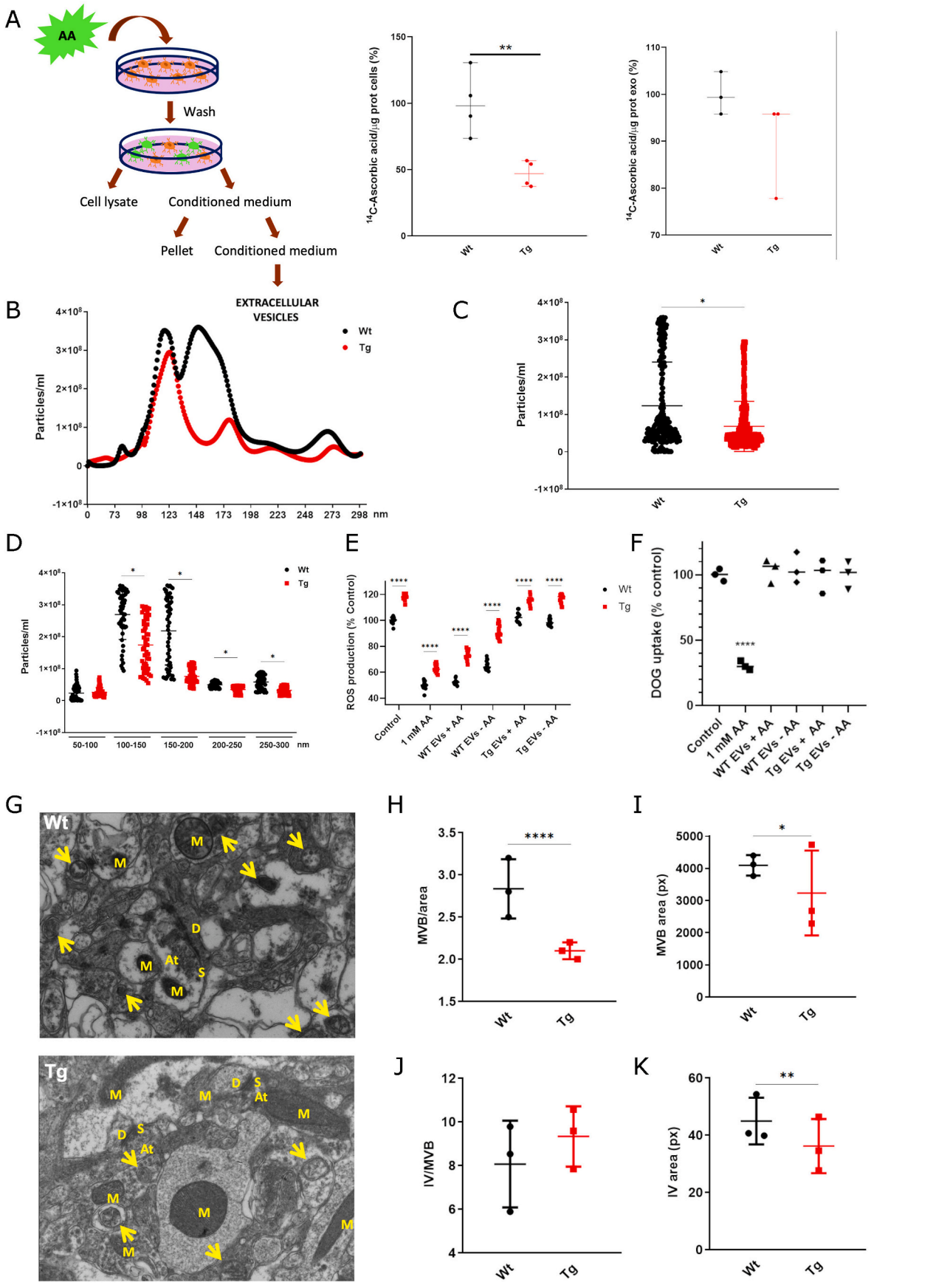

(caption on next page)

Fig. 8. YAC128 mice exhibit altered MVB biogenesis, which impairs secretion of EVs loaded with ascorbic acid. A. Left: Schematic representation of Ascorbic acid (AA) uptake experiments. YAC128 and WT primary striatal astrocyte cultures were loaded with ^{14}C-AA as described in the methods. Right: Cell culture media was collected, and cells were lysed for ^{14}C-AA detection in cells and EVs. **B.** Size distribution of YAC128 and WT primary astrocyte-derived EVs. **C.** Total particle count in EVs shown in the left panel. **D.** Total particle count per size interval. Exosomal fractions mainly contain particles between 100 and 200 nm. **E.** ROS production in primary cultures of neurons obtained from YAC128 embryos (WT or Tg). Cells were preincubated with 1 mM ascorbic acid (AA) or extracellular vesicles obtained from primary astrocytes derived from YAC128 mice (WT or Tg). Astrocyte cultures were either pre-treated (EV + AA) or not (EV-AA) with 1 mM ascorbic acid for 60 min at 37 °C before obtaining extracellular vesicles **F.** ^{3}H-deoxyglucose (DOG) transport analysis using a 10-sec uptake assay (37 °C) in primary cultures of neurons. Cells were preincubated for 15 min with 1 mM ascorbic acid (AA) or extracellular vesicles obtained from primary astrocytes derived from YAC128 mice (WT or Tg). Astrocyte cultures were either pre-treated (EV + AA) or not (EV-AA) with 1 mM ascorbic acid for 60 min at 37 °C before obtaining extracellular vesicles **G.** Transmission electron microscopy in YAC128 (left) and control (right) dorsal striatum preparations. Highlights: MVBs (arrows), Mitochondria (M), Axon terminal (At) and Synapses (S). **H.** MVB count per analyzed area. **I.** MVB range. **J.** IV count per MVB. **K.** IV range. Student's t-test, n = 4 for every condition (A), $^{**}p < 0.01$. Student's t-test, n = 4 for every condition (C, D), $^{*}p < 0.05$. One-way ANOVA followed by the Tukey post-test, n = 3 for every condition, $^{****}p < 0.0001$ (E). One-way ANOVA followed by the Dunnet post-test, n = 3 for every condition, $^{****}p < 0.0001$ (F). Student's t-test, n = 3 for every condition (H–K), $^{*}p < 0.05$, $^{****}p < 0.0001$.

compensatory response, but GFAP-HD160Q mice do not. This should be because GFAP-HD160Q mice express wild-type Htt in neurons, while mutant Htt is exclusively present in astrocytes. Decreased expression of GLUT3 has been described in other neurodegenerative diseases, such as Alzheimer's disease [80] and transmissible spongiform encephalopathies [81], and higher GLUT3 copy-numbers delay HD age of onset [82] suggesting glucose metabolism is altered in HD.

In conclusion, we found that astrocytic ascorbic acid release is impaired in presymptomatic mouse models of HD. When the glutamatergic corticostriatal pathway is activated, astrocytes remove glutamate from the synaptic cleft (Fig. 9), which stimulates them to release lactate and ascorbic acid. We observed fewer MVBs in the striatum of HD mice, and our data suggest ascorbic acid is released in part through exosomes; however, we cannot discard ascorbic acid release via ectosomes and other mechanisms delivering "free" ascorbic acid. Neurons could take up ascorbic acid released via fusion of EVs with their plasma membrane, receptor-mediated EV endocytosis, or SVCT2. "Free" ascorbic acid taken up through SVCT2 stimulates lactate uptake favoring optimal energy production while ascorbic acid released through extracellular vesicles and then taken up by neurons is used to maintain redox balance. Synaptic activity produces oxidant species that oxidize ascorbic acid to dehydroascorbic acid (DHA), which is released from neurons and taken up by astrocytes that reduce DHA to ascorbic acid via glutathione-dependent reductases. Our results demonstrate that ascorbic acid homeostasis is altered before the onset of overt HD-like behavioral symptoms and that impaired ascorbic acid release from astrocytes is Htt-dependent. Studies like this, which explore early cellular and molecular mechanisms before the onset of HD, can serve as a foundation for designing preventive therapeutic strategies, particularly given that HD is a genetic and progressive condition.

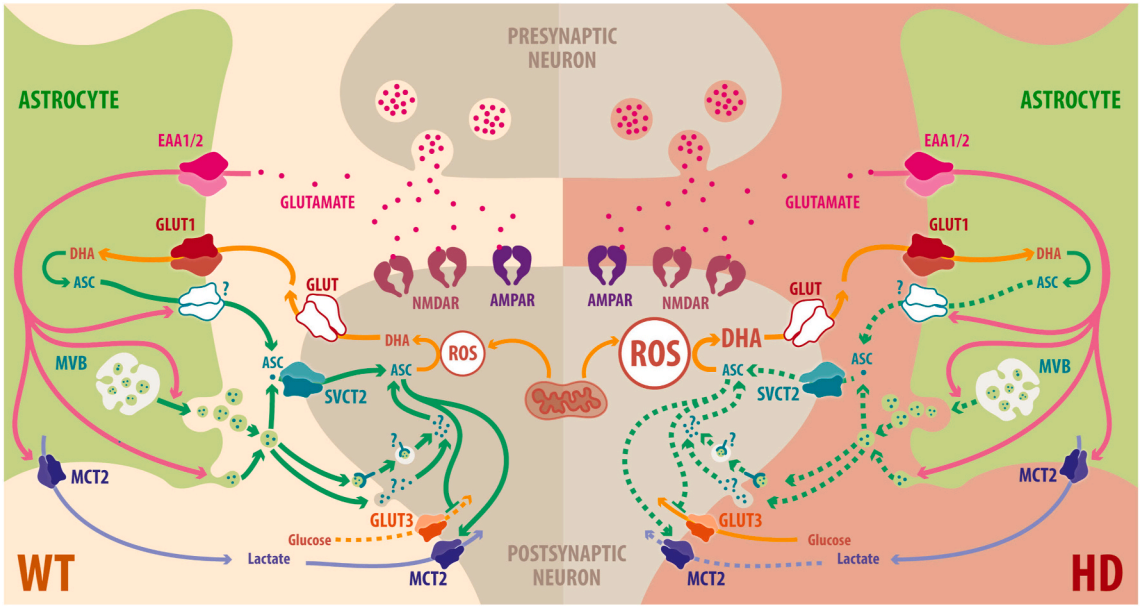

Fig. 9. EVs-mediated ascorbic acid release from HD astrocytes is impaired and alters neuronal energy substrate preferences. WT: During corticostriatal pathway activation, glutamate is released into the synaptic cleft. Astrocytes take up glutamate, which stimulates them to release lactate and ascorbic acid. Ascorbic acid is released from astrocytes in EVs (exosomes and/or ectosomes) or freely through an unknown mechanism. Neurons could absorb it via the fusion of EVs with the plasma membrane, receptor-mediated EV endocytosis, and SVCT2 mediated transport. Intracellular ascorbic acid absorbed by SVCT2 transport inhibits glucose consumption by inhibiting GLUT3 and stimulates lactate uptake in neurons. Synaptic activity requires ATP production by oxidative metabolism which produces reactive oxidant species (ROS). Intracellular ascorbic acid prevenient from EVs is oxidized to dehydroascorbic acid (DHA) to maintain redox balance. DHA is released from neurons and taken up by astrocytes via glucose transporters. Astrocytes can reduce oxidized ascorbic acid because they express specific glutathione-dependent reductases. **HD:** MVB biogenesis is impaired in astrocytes expressing mHtt; therefore, they secrete fewer ascorbic acid-containing exosomes and ectosomes. In presymptomatic stages of HD, reduced ascorbic acid release from astrocytes cells alters redox balance and then impaire neuronal energy metabolism. AMPAR, (2-amino-3-(3-hydroxy-5-methyl-isoxazole-4-yl)propanoic acid receptor; Asc, ascorbic acid; DHA, dehydroascorbic acid, oxidized ascorbic acid; EAAT, excitatory amino acid transporter; GLUT3, glucose transporter isoform 3; GSH, reduced glutathione; GSSG, oxidized glutathione; NMDAR, N methyl-D-aspartate receptor; MCT, monocarboxylate transporter; ROS, reactive oxygen species; SVCT2, sodium-vitamin C transporter isoform 2.

4. Materials and methods

Animals. YAC128 (Jackson Laboratory, stock number Stock No: 004938, male, 2–3 months old) mice maintenance and breeding were done in the Veterinary Pharmacology and Morphophysiology Institute of the Veterinary Sciences Faculty Animal Facility of Universidad Austral de Chile. Animals were maintained in a 12:12 light: dark cycle and supplied with commercial food pellets and water ad libitum. Genotyping was performed by PCR following The Jackson Laboratory protocol. GFAP-HD160Q (Jackson Laboratory, stock number Stock No: 012630, male, 3–6 months old) mice were also bred and maintained at the Veterinary Pharmacology and Morphophysiology Institute of the Veterinary Sciences Faculty Animal Facility of Universidad Austral de Chile. Animals were maintained in a 12:12 light: dark cycle and supplied with commercial food pellets and water ad libitum. Genotyping was performed by conventional PCR to determine polyglutamine repetitions (Bradford el at., 2009). All experiments were conducted in accordance with the Chilean Government's Manual of Bioethics and Biosafety (ANID: The National Research and Development Agency, Santiago, Chile) and according to the guidelines established by the Animal Protection Committee of the Universidad Austral de Chile.

Slice preparation. Mice were anesthetized with isoflurane (1-chloro-2,2,2-trifluoroethyl difluoromethyl ether) before decapitation. Brains were removed and placed into ice-cold low-Ca2 oxygenated artificial cerebrospinal fluid (ACSF: 130 mM NaCl, 5 mM $MgCl_2$, 1 mM $CaCl_2$, 3 mM kC, 1.25 mM NaH_2PO_4, 26 mM $NaHCO_3$ and 10 mM glucose). Coronal slices (350 μm) were prepared using a vibrotome T1200 (Leica). Slices containing the striatum and overlying cortex were maintained at room temperature in an incubation chamber filled with ACSF that was bubbled continuously with 95 % O_2–5% CO_2 for 1 h before being transferred to a thin-layer laminar flow submersion recording chamber.

Electrophysiological assays. Excitatory postsynaptic field potentials (fEPSPs, extracellular field excitatory postsynaptic potentials) were recorded and evoked using a bipolar electrode positioned in the corpus callosum to preferentially activate glutamatergic cortical afferents**.** Field potentials were recorded in the dorsolateral striatum using an Axopatch 200B with a Digidata 1200 amplifier (Axon Instruments), or a Microelectrode AC Amplifier Model 1600 (A-M Systems) with acquisition card PCI-6014 (National Instruments). Glass pipettes were pulled in a P-87 Puller (Sutter Instruments, Novato CA) having 1–2 MΩ resistance and filled with ACSF. Signal were digitized at 25 Khz and analyzed with WinWCP software. Field potentials were evoked with 200 μs long current pulses at 50 % of maximal fEPSP amplitude, every 30 s. A paired-pulse separated by intervals of 20, 50, 100 or 200 ms was applied to obtain the paired pulse ratio (PPR), dividing the amplitudes of the second over the first pulse. Response recovery after glucose deprivation was analyzed using ACSF containing sucrose instead of glucose (ACSF with 5 mM sucrose, 2 mM CaCl2, and 2 mM MgCl2, pH 7.2–7.4, 290–310 mOsm) in the presence or absence of the inhibitor of monocarboxylate transporters α-cyano-4-hydroxycinnamate (4-CIN) and/or 0.5 mM ascorbic acid in the presence of 0.1 Mm DTT, depending on the experiment**.**

Quantitative reverse transcription real-time PCR. RNA was extracted from samples with the EZNA Total RNA Kit II (Omega Bio-Tek, Norcross, GA, USA) according to the manufacturer's protocol. RNA quantification and purity were analyzed with a spectrophotometer. cDNA was synthesized using the Maxima Universal First Strand cDNA Synthesis Kit (Thermo Fisher Scientific, Rockford, IL, USA). PCR was performed using the Maxima SYBR Green qPCR Master Mix (Thermo Fisher Scientific). The following primers were used to analyse: SVCT2, sense: 5′ atg atg ggt atc ggc aag aac a 3′ and antisense: 5′ gct ccg tgt cct cgt tgt c 3'; GLUT1, sense: 5′ ggg ggc atg att ggt tcc tt 3′ and ntisense: 5′ taa gca cag cag cca caa ag 3'; GLUT3, sense: 5′ tca tct tcg ctg cct tcc tca 3′ and antisense: 5′ cag cac tca gaa gca gtc ctg gt 3'; MCT1, sense: 5′ gca acg acc agt gaa gta tc 3′ and antisense: 5′ gca acc aga cag aca acc a 3'; MCT2, sense: 5′ ggg ctg ggt cgt agt ctg t 3′ and antisense: 5′ atc caa gcg atc tga ctg gag 3'; MCT4, sense: 5′ cac ggg ttt ctc cta cgc c 3′ and antisense: 5′ gct gta gcc aat ccc aaa ctc 3'; glutharedoxine, sense: 5′ gct cag gag ttt gtg aac tgc 3′ and antisense: 5′ aga aga cct tgt ttg aaa ggc a 3'; thioredoxine, sense: 5′ ccc act tgc ccc aac tgt t 3′ and antisense: 5′ ggg agt gtc ttg gag gga c 3'.

Western blot analysis. Total protein extracts were obtained from YAC128 or GFAP-HD160Q mice striatum and primary cell cultures. Dissected striatum were homogenized in buffer A, (2 μg/ml pepstain A, 2 μg/ml leupeptin, and 2 μg/ml aprotinin) and sonicated three to five times for 10 s at 4 °C. Proteins were resolved by SDS–PAGE (70 mg per lane for total protein extract) in a 10 % (w/v) polyacrylamide gel, transferred to polyvinylidene difluoride membranes (0.45-mm pore; Amersham Pharmacia Biotech., Piscataway, NJ, USA) and probed with anti-Alix (1:200, sc-49267, Santa Cruz Biotechnology, Santa Cruz, CA, USA), anti-CD-63 (1:100, sc-15363, Santa Cruz Biotechnology, Santa Cruz, CA, USA) anti-b actin (1:1,000, sc-81178, Santa Cruz Biotechnology, Santa Cruz, CA, USA), anti-Huntingtin (1:1,000, MAB2166, Chemicon Millipore/Sigma-Aldrich Corp. St Louis, MO, USA), anti-Bip (1:1,000, sc-1050, Santa Cruz Biotechnology, Santa Cruz, CA, USA), and anti-GAPDH antibodies (1:1,000, sc-25778). The reaction was developed using anti-mouse, anti-rabbit, anti-goat HRP, conjugated antibodies (1:1,000, PA1-86326 and 31430, Thermo Scientific, Rockford, IL, USA) and the enhanced chemiluminescence Western blot method (Amersham Biosciences, Pittsburgh, PA, USA).

Primary cultures: *Astrocytes:* Striatal astrocytes were obtained from 1 to 3-day-old newborn YAC128 or GFAP-HD160Q mice, as described previously. Newborn forebrains were removed, and the striatum were dissected. Striatal tissue was digested with 0.12 % trypsin (w/v, Gibco Co., Rockville, MD, USA) in 0.1 M phosphate buffer (PBS: pH 7.4, osmolarity 320 mOsm) and mechanically disrupted with a fire-polished Pasteur pipette. Cells were plated at 0.3 × 106 cells per cm2 in plates onto coverslips coated with poly-L-lysine (mol. Wt 4350 kDa, Sigma-Aldrich Corp. St Louis, MO, USA). After 20 min, floating cells were removed, and attached cells were cultured for 5–7 days in neurobasal medium (Gibco) supplemented with B27 (Gibco), 50 U ml^{-1} penicillin, 50 mg/ml streptomycin, 50 ng ml^{-1} amphotericin B and 2 mM L-glutamine (Nalgene). *Neurons:* Striatal neurons were obtained from 17-day-old embryos of YAC128 mice, following the procedure outlined by Acuña et al. (2013). Adult female rats were anesthetized using isoflurane (1-chloro-2,2,2-trifluoroethyl difluoromethyl ether), and the forebrains of embryos were surgically removed to isolate the striatum. The dissected tissue was then treated with 0.12 % trypsin (w/v, Gibco Co., Rockville, MD, USA) in 0.1 M phosphate buffer (PBS: pH 7.4, osmolarity 320 mOsm) and mechanically dissociated using a fire-polished Pasteur pipette. The resulting cells were plated at a density of 0.3 × 106 cells per cm2 onto poly-L-lysine-coated coverslips. After 20 min, floating cells were discarded, and the remaining attached cells were cultured for 5–7 days in neurobasal medium (Gibco) supplemented with B27 (Gibco), 50 U ml^{-1} penicillin, 50 mg/ml streptomycin, 50 ng ml^{-1} amphotericin B, and 2 mM L-glutamine (Nalgene).

Ascorbic acid recycling and efflux experiments. Primary cultures of striatal astrocytes from YAC 128 mice and their controls were plated at 6-8 ×104 cells per cm2 in 12-well plates for both experiments. In efflux experiments, cells were incubated with 1 mM ascorbic acid and 0.1 mM DTT in incubation buffer for 30 min at 37 °C. Subsequently, incubation buffer was replaced by 0.5 mM L-glutamate and 0.1 mM DTT and cells were settled at 37 °C in a CO2 incubator. The culture solution was removed, and 1 μl of 100 mM DTT was added to avoid oxidation of ascorbic acid. In ascorbic acid recycling experiments, DHA was obtained from Ascorbate Oxidase enzyme oxidation of ascorbic acid (1 unit of enzyme for each μmol of ascorbic acid) at 37 °C for 10 min in incubation buffer. Cells were incubated with 0.5 mM DHA at 37 °C for 30 min, then replaced by incubation buffer containing 0.5 mM L-glutamate and 0.1 mM DTT. Cells were settled for another 30 min at 37 °C in a CO2 incubator. Cells were then lysed in 300 mM NaCl, 50 mM Tris-HCl pH 6.8, 0.5 % Triton X-100 buffer and metaphosphoric acid was added to a

final concentration of 0.7 mM and 1 mM DTT at 4 °C for 15 min in the dark. The cell lysate was centrifuged at 10,000×*g* for 10 min at 4 °C, and the supernatant was immediately filtered through a 0.22 μm filter and injected into the HPLC for chromatographic analysis.

Ascorbic acid HPLC analyses. HPLC was performed using an Agilent C18 column (Zorbax Eclipse XDB-C18, Agilent). The gradient times were as follows: 0–5 min (100 % Formic acid 0,1 % water diluted), 5–15 min (50 % Formic acid 0,1 % water diluted, 50 % Formic acid 0,1 % acetonitrile diluted), 15–17 min (5 % de Formic acid 0,1 % water diluted, 95 % Formic acid 0,1 % acetonitrile diluted), 17–25 min (Formic acid 0,1 % water diluted). Ascorbic acid standard solution was prepared at 100 mM in 1 mM DTT, Hepes 15 mM, NaCl 135 mM, KCl 5 mM, $CaCl_2$ 1,8 mM, $MgCl_2$ 0,8 mM, 320 mOsm, pH 7,4. All samples were filtered through a 0.22 μm filter (PVDF). 100 μL of each sample was injected onto the column.

GSH/GSSG detection. For Glutathione detection, a commercial GSH/GSSG-GloTM Assay kit was used (Promega, USA). Primary cell cultures were seeded in 96-well plates at a density of 6–8 x 104 cells/cm2 24 h before the experiment. The cell culture medium was removed for the test, and cells were lysed with 25 μl of total glutathione lysis solution (Total Glutathione Lysis Reagent) or with 25 μl of Oxidized Glutathione Lysis Reagent. Plates were shaken at 400 rpm for 5 min, then 25 μl of Luciferin Generation Reagent was added, and plates were incubated for 30 min at room temperature. Finally, 50 μl of detection reagent (Luciferin Detection Reagent) was added, and then plates were shaken and allowed to equilibrate for 15 min. Luminescence was quantified in a plate reader device.

EV harvesting. Cells were cultivated using EV-free medium. EV-free medium was prepared using EV-free FBS. EV-free FBS was obtained form the supernatant after ultracentrifugation at 100,000×*g* for 16 h at 4 °C. 24-hour cell culture medium was collected from plates to perform differential centrifugation at 10,000×*g* for 60 min at 4 °C. The supernatant was filtered through a 0.22 μm filter and ultracentrifuged at 100,000×*g* for 16 h at 4 °C. The supernatant was discarded, and the pellet was washed with 20 mM HEPES Buffer and ultracentrifuged again at 100,000×*g* for 16 h at 4 °C. The supernatant was then discarded, and the exosome enriched pellet was resuspended in 0.1 M phosphate buffer (PBS: pH 7.4, osmolarity 320 mOsm) diluted in ultra-pure water.

Nanoparticle tracking analysis. Samples were prepared as described in EV harvesting and analyzed by monitoring nanoparticles using a Nanosight S300®. 1 ml of PBS, PBS + Wild type samples or PBS + YAC 128 samples were injected into an automated positioning cell. Parameters such as particle size and concentration were recorded, automatically analyzed, and representative histograms of the concentration and populations of particles were plotted using the Malvern® software included in the equipment.

Scanning Electron Microscopy. EVs were pelleted from cell culture supernatants as described above, and the pellet was suspended in 100 μL of PBS. Aliquots of 30 μL were placed on 13-mm round coverslips previously treated with Biobond and allowed to adhere for 30 min. EVs were rinsed in PBS, treated with 0,1 M cacodylate buffer at 4 °C overnight and postfixed in 1 % osmium tetroxide (EM Sciences) for 2 h. Samples were rinsed in Milli-Q water (pH 7) and stored at 4 °C overnight. EVs were incubated in saturated thiocarbohydrazide solution (EM Sciences) for 10 min, rinsed in Milli-Q water and incubated in 1 % osmium tetroxide for 30 min. EVs were then rinsed in Milli-Q (pH 7) and mounted on water immersed support. EVs were dehydrated in Ethanol PA (Merck) as follows: 30 % (5 min); fifty% (5 min); 70 % (5 min); 90 % (5 min); 100 % (10 min); 100 % (10 min) and then were critically point-dried. The coverslips were mounted on aluminum stubs with silver paint (EM Sciences). Finally, samples were coated with gold vapor for 40 min and analyzed in a JEOL JSM6610LV electron microscope (JEOL, Tokyo, Japan).

Transmission Electron Microscopy. Mice were perfused intravascularly with 0.5 % glutaraldehyde and 4 % paraformaldehyde in 30 mM HEPES, 100 mM NaCl (pH 7.4). Brains were removed, and the two hemispheres were separated, fixed for 2 h in the same fixative, postfixed in OsO_4, and embedded in Epon resin (EMbed-812; EMS). Only the dorsal section of the striatum was used. Ultrathin sections were stained with uranyl acetate and lead citrate and examined on an EM Zeiss EM900 electron microscope in the Advanced microscopy unit (UMA) of the Biological Sciences Faculty of Pontificia Universidad Católica de Chile.

KD-Htt HEK cells generation. Our KD-Htt HEK cell line was generated using a CRISPR-Cas9 approach. Two targets were chosen at 5' region of Htt gen and two pairs of guide RNA (sgRNA) were designed: sgRNA-htt-A: CAACTCTTCGCATCCTGCGA and sgRNA-htt-B: ATTTGCGAGAAACCAGGGCG. sgRNAs were cloned into a pU6-Puro vector. Plasmid DNA was purified, and positive clones were sequenced. For the ablation of Htt, HEK293T cells were transfected with 2 μg Cas9 D10A + 2 μg sgRNA mixture 1:1, using OPTIMEM™ and Lipofectamine 2000™. Cells were incubated for 12 h in DMEM culture medium supplemented with 10 % Fetal Bovine Serum, 2 mM L-glutamine and 50 mg/ml Normocine (Invitrogen), transfected cells were selected 48h with 4 μg/ml puromycin and further individual clones were isolated and tested for htt ablation.

Uptake assays. Uptake assays were conducted in 400 μl of incubation buffer (IB) consisting of 15 mM Hepes (pH 7.4), 135 mM NaCl, 5 mM KCl, 1.8 mM $CaCl_2$, and 0.8 mM $MgCl_2$, supplemented with 0.1 ± 0.4 mCi of 1±^{14}C-L-ascorbic acid (specific activity: 8.2 mCi mmol-1, Dupont NEN). Uptake was terminated by rinsing cells with ice-cold IB containing 0.2 mM $HgCl_2$. Cells were lysed in 200 μl of lysis buffer (10 mM Tris–HCl, pH 8.0, with 0.2 % SDS), and the incorporated radioactivity was quantified using liquid scintillation spectrometry[22]. Before uptake, cells were preincubated with either 0 (control), 1 mM ascorbic acid, or EVs (the extracellular vesicles obtained from a 55 cm^2 culture dish of astrocytes were added to a well with an area of 4 cm^2 containing neurons) diluted in IB containing 0.1 mM DTT for 30 min.

ROS determination in living cells. Reactive oxygen species (ROS) production was assessed by measuring the oxidation of DCFH-DA (2′, 7′-dichlorofluorescein diacetate) to fluorescent DCF, following a method previously described by Covarrubias-Pinto et al., 2015. Cells were seeded onto 96-well plates at a density of 1.5 × 10⁴ cells per well and preincubated with either 0 1 mM ascorbic acid, or EVs (the 2/25th of extracellular vesicles obtained from a 55 cm^2 culture dish of astrocytes were added to a well with an area of 0.32 cm^2 containing neurons) diluted in IB containing 0.1 mM DTT for 30 min. Subsequently, 5 μg/ml DCFH-DA was added, and fluorescence intensity was measured using a Synergy 2 Multi-Mode microplate reader equipped with filters for 485 nm excitation and 520 nm emission. Relative fluorescence units (RFU) were recorded at 40-s intervals over a 10-min period.

C^{14}-ascorbic acid efflux assay. Primary astrocytes were incubated in an EV-free culture medium supplemented with 1 mM ascorbic acid (AA) and 9,35 μM C^{14}-AA **for** 3 h. The incubation medium was then washed, and cell plates were settled with fresh EV-free medium for 24 h. The cell culture medium was then collected and centrifuged at 10.000 g for 1 h at 4 °C. Cells were then treated with 0,12 % trypsin buffer for 15 min at 37 °C and lysed for 30 min with Tris-HCl 10 mM pH 8,0, SDS 0,2 % buffer with protease inhibitor (Thermo Fisher Scientific, Rockford, IL, USA) at 4 °C for cell counting, protein quantification and radioactivity counting. After centrifugation, the cell culture medium was collected and filtered through a 0.22 μm filter and ultracentrifuged at 100.000 g for 16 h at 4 °C for EV harvesting. After ultracentrifugation, the supernatant was collected and lysed for 30 min for radioactivity counting, and the pellet was washed with 20 mM Hepes Buffer and ultracentrifuged again at 100,000×*g* for 16 h at 4 °C. After the second round of ultracentrifugation, the supernatant was discarded, and the pellet was resuspended in 20 mM Hepes Buffer and lysed for 30 min. EV radioactivity count was performed using Ecoscint biodegradable scintillation liquid, and measurements were taken by a PerkinElmer Tri-Carb 2910 TR liquid scintillation counter. All assays using radioisotopes were carried out in accordance with the biosafety measures of the 2008

CONICYT ″ Biosafety Standards Manual ". The contaminated waste was stored in special warehouses destined for it in the facilities of the University's Environmental Management Unit (UGA)., according to the University's Waste Management Procedure Manual.

Statistical analyses. Statistical comparison between two or more data groups was performed using Student's t-test or analysis of variance (ANOVA) followed by the Bonferroni post-test.

CRediT authorship contribution statement

Felipe A. Beltrán: Investigation. **Leandro Torres-Díaz L.:** Investigation. **Paulina Troncoso-Escudero:** Investigation. **Juan Villalobos-González:** Investigation. **Gonzalo Mayorga-Weber:** Investigation. **Marcelo Lara:** Investigation. **Adriana Covarrubias-Pinto:** Investigation. **Sharin Valdivia:** Investigation. **Isidora Vicencio:** Investigation. **Eduardo Papic:** Investigation. **Carolina Paredes-Martínez:** Investigation. **Mara E. Silva-Januàrio:** Investigation. **Alejandro Rojas:** Methodology, Investigation. **Luis L.P. daSilva:** Methodology, Investigation. **Felipe Court:** Methodology, Investigation. **Abraham Rosas-Arellano:** Methodology, Investigation. **Luis Federico Bátiz:** Resources, Methodology, Investigation. **Patricio Rojas:** Methodology, Investigation. **Francisco J. Rivera:** Writing – review & editing, Writing – original draft, Resources, Project administration, Methodology, Investigation, Funding acquisition, Formal analysis, Data curation, Conceptualization. **Maite A. Castro:** Writing – review & editing, Writing – original draft, Supervision, Resources, Project administration, Methodology, Investigation, Funding acquisition, Conceptualization.

Data availability statement

Data used to prepare figures are available at https://www.dropbox.com/scl/fo/n71e95tk2jfzpvii7l7hp/ABT4YnmWogEKA3NOp9NVb9M?rlkey=q7hpallqel9kuyehlsq941t1u&dl=0.

Declaration of competing interest

The authors declare that they have no known competing financial interests or personal relationships that could have appeared to influence the work reported in this paper.

Acknowledgments

This work was supported by the Chilean FONDECYT grant 1151206 (MAC), 1191620 (MAC), Chilean CONICYT-REDES grant 180139 (MAC), FONDECYT grant 1201706 (FJR), Janelia Visitor Program JVS0028700 (MAC), DICYT-USACH (PR), FONDECYT grant 1211384 (LFB) and International SfA grant (MAC). In addition, thanks to PROFI 6 N° 336,234 of the Research Council of Finland.

References

[1] M.S. Haddad, J.L. Cummings, Huntington's disease, Psychiatr Clin North Am 20 (4) (1997) 791–807.
[2] M. Pennuto, I. Palazzolo, A. Poletti, Post-translational modifications of expanded polyglutamine proteins: impact on neurotoxicity, Hum. Mol. Genet. 18 (R1) (2009) R40–R47.
[3] E. Cattaneo, D. Rigamonti, D. Goffredo, C. Zuccato, F. Squitieri, S. Sipione, Loss of normal huntingtin function: new developments in Huntington's disease research, Trends Neurosci. 24 (3) (2001) 182–188.
[4] T.M. Greco, C. Secker, E.S. Ramos, J.D. Federspiel, J.P. Liu, A.M. Perez, et al., Dynamics of huntingtin protein interactions in the striatum identifies candidate modifiers of Huntington disease, Cell Syst 13 (4) (2022), 304-320 e5.
[5] P. Hilditch-Maguire, F. Trettel, L.A. Passani, A. Auerbach, F. Persichetti, M. E. MacDonald, Huntingtin: an iron-regulated protein essential for normal nuclear and perinuclear organelles, Hum. Mol. Genet. 9 (19) (2000) 2789–2797.
[6] J. Velier, M. Kim, C. Schwarz, T.W. Kim, E. Sapp, K. Chase, et al., Wild-type and mutant huntingtins function in vesicle trafficking in the secretory and endocytic pathways, Exp. Neurol. 152 (1) (1998) 34–40.
[7] G. Hoffner, P. Kahlem, P. Djian, Perinuclear localization of huntingtin as a consequence of its binding to microtubules through an interaction with beta-tubulin: relevance to Huntington's disease, J. Cell Sci. 115 (Pt 5) (2002) 941–948.
[8] J.P. Caviston, E.L. Holzbaur, Huntingtin as an essential integrator of intracellular vesicular trafficking, Trends Cell Biol. 19 (4) (2009) 147–155.
[9] S. Finkbeiner, Huntington's disease, Cold Spring Harbor Perspect. Biol. 3 (6) (2011).
[10] B.K. Siesjo, Brain energy metabolism and catecholaminergic activity in hypoxia, hypercapnia and ischemia, J. Neural. Transm. Suppl. (14) (1978) 17–22.
[11] A. Tramutola, H.S. Bakels, F. Perrone, M. Di Nottia, T. Mazza, M.P. Abruzzese, et al., GLUT-1 changes in paediatric Huntington disease brain cortex and fibroblasts: an observational case-control study, EBioMedicine 97 (2023) 104849.
[12] I.J. Mitchell, R. Luquin, S. Boyce, C.E. Clarke, R.G. Robertson, M.A. Sambrook, et al., Neural mechanisms of dystonia: evidence from a 2-deoxyglucose uptake study in a primate model of dopamine agonist-induced dystonia, Mov. Disord. 5 (1) (1990) 49–54.
[13] K. Leenders, Positron emission tomography with labelled l-dopa and methispiperone in patients with movement disorders, Biol. Psychol. 21 (1985) 273.
[14] F. Mochel, R.G. Haller, Energy deficit in Huntington disease: why it matters, J. Clin. Invest. 121 (2) (2011) 493–499.
[15] H. Ischiropoulos, J.S. Beckman, Oxidative stress and nitration in neurodegeneration: cause, effect, or association? J. Clin. Invest. 111 (2) (2003) 163–169.
[16] G.V. Rebec, S.K. Conroy, S.J. Barton, Hyperactive striatal neurons in symptomatic Huntington R6/2 mice: variations with behavioral state and repeated ascorbate treatment, Neuroscience 137 (1) (2006) 327–336.
[17] G.V. Rebec, S.J. Barton, A.M. Marseilles, K. Collins, Ascorbate treatment attenuates the Huntington behavioral phenotype in mice, Neuroreport 14 (9) (2003) 1263–1265.
[18] M.A. Castro, F.A. Beltran, S. Brauchi, I.I. Concha, A metabolic switch in brain: glucose and lactate metabolism modulation by ascorbic acid, J. Neurochem. 110 (2) (2009) 423–440.
[19] M.A. Castro, C. Angulo, S. Brauchi, F. Nualart, I.I. Concha, Ascorbic acid participates in a general mechanism for concerted glucose transport inhibition and lactate transport stimulation, Pflugers Arch 457 (2) (2008) 519–528.
[20] M.A. Castro, M. Pozo, C. Cortes, L. Garcia Mde, I.I. Concha, F. Nualart, Intracellular ascorbic acid inhibits transport of glucose by neurons, but not by astrocytes, J. Neurochem. 102 (3) (2007) 773–782.
[21] J.X. Wilson, C.E. Peters, S.M. Sitar, P. Daoust, A.W. Gelb, Glutamate stimulates ascorbate transport by astrocytes, Brain Res. 858 (1) (2000) 61–66.
[22] M. Castro, T. Caprile, A. Astuya, C. Millan, K. Reinicke, J.C. Vera, et al., High-affinity sodium-vitamin C co-transporters (SVCT) expression in embryonic mouse neurons, J. Neurochem. 78 (4) (2001) 815–823.
[23] M. Solis-Maldonado, M.P. Miro, A.I. Acuna, A. Covarrubias-Pinto, A. Loaiza, G. Mayorga, et al., Altered lactate metabolism in Huntington's disease is dependent on GLUT3 expression, CNS Neurosci. Ther. 24 (4) (2018) 343–352.
[24] A.I. Acuna, M. Esparza, C. Kramm, F.A. Beltran, A.V. Parra, C. Cepeda, et al., A failure in energy metabolism and antioxidant uptake precede symptoms of Huntington's disease in mice, Nat. Commun. 4 (2013) 2917.
[25] A. Astuya, T. Caprile, M. Castro, K. Salazar, L. Garcia Mde, K. Reinicke, et al., Vitamin C uptake and recycling among normal and tumor cells from the central nervous system, J. Neurosci. Res. 79 (1–2) (2005) 146–156.
[26] R.D. O'Neill, M. Fillenz, L. Sundstrom, J.N. Rawlins, Voltammetrically monitored brain ascorbate as an index of excitatory amino acid release in the unrestrained rat, Neurosci. Lett. 52 (3) (1984) 227–233.
[27] M.A. Hediger, New view at C, Nat Med. 8 (5) (2002) 445–446.
[28] M.E. Rice, Ascorbate regulation and its neuroprotective role in the brain, Trends Neurosci. 23 (5) (2000) 209–216.
[29] C.R. Rose, B.R. Ransom, Intracellular sodium homeostasis in rat hippocampal astrocytes, J Physiol. 491 (Pt 2) (1996) 291–305. Pt 2.
[30] J. Bradford, J.Y. Shin, M. Roberts, C.E. Wang, X.J. Li, S. Li, Expression of mutant huntingtin in mouse brain astrocytes causes age-dependent neurological symptoms, Proc. Natl. Acad. Sci. U.S.A. 106 (52) (2009) 22480–22485.
[31] L. Mangiarini, K. Sathasivam, M. Seller, B. Cozens, A. Harper, C. Hetherington, et al., Exon 1 of the HD gene with an expanded CAG repeat is sufficient to cause a progressive neurological phenotype in transgenic mice, Cell 87 (3) (1996) 493–506.
[32] J. Kaye, T. Reisine, S. Finkbeiner, Huntington's disease mouse models: unraveling the pathology caused by CAG repeat expansion, Fac Rev. 10 (2021) 77.
[33] G. Nittari, P. Roy, I. Martinelli, V. Bellitto, D. Tomassoni, E. Traini, et al., Rodent models of Huntington's disease: an overview, Biomedicines 11 (12) (2023).
[34] E.J. Slow, J. van Raamsdonk, D. Rogers, S.H. Coleman, R.K. Graham, Y. Deng, et al., Selective striatal neuronal loss in a YAC128 mouse model of Huntington disease, Hum. Mol. Genet. 12 (13) (2003) 1555–1567.
[35] K. Pierre, P.J. Magistretti, L. Pellerin, MCT2 is a major neuronal monocarboxylate transporter in the adult mouse brain, J. Cerebr. Blood Flow Metabol. 22 (5) (2002) 586–595.
[36] S. Brauchi, M.C. Rauch, I.E. Alfaro, C. Cea, I.I. Concha, D.J. Benos, et al., Kinetics, molecular basis, and differentiation of L-lactate transport in spermatogenic cells, Am. J. Physiol. Cell Physiol. 288 (3) (2005) C523–C534.
[37] A.P. Halestrap, N.T. Price, The proton-linked monocarboxylate transporter (MCT) family: structure, function and regulation, Biochem. J. 343 (Pt 2) (1999) 281–299. Pt 2.
[38] S.J. Vannucci, Developmental expression of GLUT1 and GLUT3 glucose transporters in rat brain, J. Neurochem. 62 (1) (1994) 240–246.

[39] F. Maher, T.M. Davies-Hill, P.G. Lysko, R.C. Henneberry, I.A. Simpson, Expression of two glucose transporters, GLUT1 and GLUT3, in cultured cerebellar neurons: evidence for neuron-specific expression of GLUT3, Mol. Cell. Neurosci. 2 (4) (1991) 351–360.
[40] J.C. Vera, C.I. Rivas, R.H. Zhang, C.M. Farber, D.W. Golde, Human HL-60 myeloid leukemia cells transport dehydroascorbic acid via the glucose transporters and accumulate reduced ascorbic acid, Blood 84 (5) (1994) 1628–1634.
[41] J. Cammack, B. Ghasemzadeh, R.N. Adams, The pharmacological profile of glutamate-evoked ascorbic acid efflux measured by in vivo electrochemistry, Brain Res. 565 (1) (1991) 17–22.
[42] M. von Zastrow, T.R. Tritton, J.D. Castle, Exocrine secretion granules contain peptide amidation activity, Proc. Natl. Acad. Sci. U. S. A. 83 (10) (1986) 3297–3301.
[43] R. Siushansian, S.J. Dixon, J.X. Wilson, Osmotic swelling stimulates ascorbate efflux from cerebral astrocytes, J. Neurochem. 66 (3) (1996) 1227–1233.
[44] S. Ahmad, W.H. Evans, Post-translational integration and oligomerization of connexin 26 in plasma membranes and evidence of formation of membrane pores: implications for the assembly of gap junctions, Biochem. J. 365 (Pt 3) (2002) 693–699.
[45] C.C. Portugal, V.S. Miya, C. Calaza Kda, R.A. Santos, R. Paes-de-Carvalho, Glutamate receptors modulate sodium-dependent and calcium-independent vitamin C bidirectional transport in cultured avian retinal cells, J. Neurochem. 108 (2) (2009) 507–520.
[46] G. van Niel, D.R.F. Carter, A. Clayton, D.W. Lambert, G. Raposo, P. Vader, Challenges and directions in studying cell-cell communication by extracellular vesicles, Nat. Rev. Mol. Cell Biol. 23 (5) (2022) 369–382.
[47] R.C. Piper, D.J. Katzmann, Biogenesis and function of multivesicular bodies, Annu. Rev. Cell Dev. Biol. 23 (2007) 519–547.
[48] J. Meldolesi, Exosomes and ectosomes in intercellular communication, Curr. Biol. 28 (8) (2018) R435–R444.
[49] G. Liot, J. Valette, J. Pepin, J. Flament, E. Brouillet, Energy defects in Huntington's disease: why "in vivo" evidence matters, Biochem. Biophys. Res. Commun. 483 (4) (2017) 1084–1095.
[50] A. Neueder, K. Kojer, T. Hering, D.J. Lavery, J. Chen, N. Birth, et al., Abnormal molecular signatures of inflammation, energy metabolism, and vesicle biology in human Huntington disease peripheral tissues, Genome Biol. 23 (1) (2022) 189.
[51] A. Tassone, M. Meringolo, G. Ponterio, P. Bonsi, T. Schirinzi, G. Martella, Mitochondrial bioenergy in neurodegenerative disease: Huntington and Parkinson, Int. J. Mol. Sci. 24 (8) (2023).
[52] J.M. Van Raamsdonk, J. Pearson, D.A. Rogers, N. Bissada, A.W. Vogl, M.R. Hayden, et al., Loss of wild-type huntingtin influences motor dysfunction and survival in the YAC128 mouse model of Huntington disease, Hum. Mol. Genet. 14 (10) (2005) 1379–1392.
[53] C. Cepeda, D.M. Cummings, V.M. Andre, S.M. Holley, M.S. Levine, Genetic mouse models of Huntington's disease: focus on electrophysiological mechanisms, ASN Neuro 2 (2) (2010) e00033.
[54] J.L. Dorner, B.R. Miller, S.J. Barton, T.J. Brock, G.V. Rebec, Sex differences in behavior and striatal ascorbate release in the 140 CAG knock-in mouse model of Huntington's disease, Behav. Brain Res. 178 (1) (2007) 90–97.
[55] A. Basse-Tomusk, G.V. Rebec, Corticostriatal and thalamic regulation of amphetamine-induced ascorbate release in the neostriatum, Pharmacol. Biochem. Behav. 35 (1) (1990) 55–60.
[56] J.M. Upston, A. Karjalainen, F.L. Bygrave, R. Stocker, Efflux of hepatic ascorbate: a potential contributor to the maintenance of plasma vitamin C, Biochem. J. 342 (Pt 1) (1999) 49–56. Pt 1.
[57] M.M. VanDuijn, K. Tijssen, J. VanSteveninck, P.J. Van Den Broek, J. Van Der Zee, Erythrocytes reduce extracellular ascorbate free radicals using intracellular ascorbate as an electron donor, J. Biol. Chem. 275 (36) (2000) 27720–27725.
[58] T. Yusa, Increased extracellular ascorbate release reflects glutamate re-uptake during the early stage of reperfusion after forebrain ischemia in rats, Brain Res. 897 (1–2) (2001) 104–113.
[59] H. Tsukaguchi, T. Tokui, B. Mackenzie, U.V. Berger, X.Z. Chen, Y. Wang, et al., A family of mammalian Na+-dependent L-ascorbic acid transporters, Nature 399 (6731) (1999) 70–75.
[60] U.V. Berger, M.A. Hediger, Distribution of the glutamate transporters GLAST and GLT-1 in rat circumventricular organs, meninges, and dorsal root ganglia, J. Comp. Neurol. 421 (3) (2000) 385–399.
[61] Ronquist K. Goran, Extracellular vesicles and energy metabolism, Clin. Chim. Acta 488 (2019) 116–121.
[62] K.A. Chamberlain, N. Huang, Y. Xie, F. LiCausi, S. Li, Y. Li, et al., Oligodendrocytes enhance axonal energy metabolism by deacetylation of mitochondrial proteins through transcellular delivery of SIRT2, Neuron 109 (21) (2021), 3456-34572 e8.
[63] K.G. Ronquist, B. Ek, J. Morrell, A. Stavreus-Evers, B. Strom Holst, P. Humblot, et al., Prostasomes from four different species are able to produce extracellular adenosine triphosphate (ATP), Biochim. Biophys. Acta 1830 (10) (2013) 4604–4610.
[64] M. Puhka, M. Takatalo, M.E. Nordberg, S. Valkonen, J. Nandania, M. Aatonen, et al., Metabolomic profiling of extracellular vesicles and alternative normalization methods reveal enriched metabolites and strategies to study prostate cancer-related changes, Theranostics 7 (16) (2017) 3824–3841.
[65] M.P. Mattson, D. Liu, Energetics and oxidative stress in synaptic plasticity and neurodegenerative disorders, NeuroMolecular Med. 2 (2) (2002) 215–231.
[66] V. Lisi, G. Senesi, N. Bertola, M. Pecoraro, S. Bolis, A. Gualerzi, et al., Plasma-derived extracellular vesicles released after endurance exercise exert cardioprotective activity through the activation of antioxidant pathways, Redox Biol. 63 (2023) 102737.
[67] H. Qi, Y. Wang, S. Fa, C. Yuan, L. Yang, Extracellular vesicles as natural delivery carriers regulate oxidative stress under pathological conditions, Front. Bioeng. Biotechnol. 9 (2021) 752019.
[68] W. Zhang, T. Wang, Y. Xue, B. Zhan, Z. Lai, W. Huang, et al., Research progress of extracellular vesicles and exosomes derived from mesenchymal stem cells in the treatment of oxidative stress-related diseases, Front. Immunol. 14 (2023) 1238789.
[69] L. Boussicault, A.S. Herard, N. Calingasan, F. Petit, C. Malgorn, N. Merienne, et al., Impaired brain energy metabolism in the BACHD mouse model of Huntington's disease: critical role of astrocyte-neuron interactions, J. Cerebr. Blood Flow Metabol. 34 (9) (2014) 1500–1510.
[70] C.V. Borlongan, T.K. Koutouzis, P.R. Sanberg, 3-Nitropropionic acid animal model and Huntington's disease, Neurosci. Biobehav. Rev. 21 (3) (1997) 289–293.
[71] R.S. Atwal, J. Xia, D. Pinchev, J. Taylor, R.M. Epand, R. Truant, Huntingtin has a membrane association signal that can modulate huntingtin aggregation, nuclear entry and toxicity, Hum. Mol. Genet. 16 (21) (2007) 2600–2615.
[72] A.M. Lopez-Guerrero, P. Tomas-Martin, C. Pascual-Caro, T. Macartney, A. Rojas-Fernandez, G. Ball, et al., Regulation of membrane ruffling by polarized STIM1 and ORAI1 in cortactin-rich domains, Sci. Rep. 7 (1) (2017) 383.
[73] F. Inesta-Vaquera, V.K. Chaugule, A. Galloway, L. Chandler, A. Rojas-Fernandez, S. Weidlich, et al., DHX15 regulates CMTR1-dependent gene expression and cell proliferation, Life Sci. Alliance 1 (3) (2018) e201800092.
[74] A. Rojas-Fernandez, A. Plechanovova, N. Hattersley, E. Jaffray, M.H. Tatham, R. T. Hay, SUMO chain-induced dimerization activates RNF4, Mol. Cell 53 (6) (2014) 880–892.
[75] A.E. Gonzalez, V.C. Munoz, V.A. Cavieres, H.A. Bustamante, V.H. Cornejo, Y. C. Januario, et al., Autophagosomes cooperate in the degradation of intracellular C-terminal fragments of the amyloid precursor protein via the MVB/lysosomal pathway, FASEB J 31 (6) (2017) 2446–2459.
[76] A.L. Nishimura, C. Shum, E.L. Scotter, A. Abdelgany, V. Sardone, J. Wright, et al., Allele-specific knockdown of ALS-associated mutant TDP-43 in neural stem cells derived from induced pluripotent stem cells, PLoS One 9 (3) (2014) e91269.
[77] A. Serio, B. Bilican, S.J. Barmada, D.M. Ando, C. Zhao, R. Siller, et al., Astrocyte pathology and the absence of non-cell autonomy in an induced pluripotent stem cell model of TDP-43 proteinopathy, Proc. Natl. Acad. Sci. U.S.A. 110 (12) (2013) 4697–4702.
[78] K.G. Bache, A. Brech, A. Mehlum, H. Stenmark, Hrs regulates multivesicular body formation via ESCRT recruitment to endosomes, J. Cell Biol. 162 (3) (2003) 435–442.
[79] A. Covarrubias-Pinto, A.V. Parra, G. Mayorga-Weber, E. Papic, I. Vicencio, P. Ehrenfeld, et al., Impaired intracellular trafficking of sodium-dependent vitamin C transporter 2 contributes to the redox imbalance in Huntington's disease, J. Neurosci. Res. 99 (1) (2021) 223–235.
[80] Y. Liu, F. Liu, K. Iqbal, I. Grundke-Iqbal, C.X. Gong, Decreased glucose transporters correlate to abnormal hyperphosphorylation of tau in Alzheimer disease, FEBS Lett. 582 (2) (2008) 359–364.
[81] Y.E. Yan, J. Zhang, K. Wang, Y. Xu, K. Ren, B.Y. Zhang, et al., Significant reduction of the GLUT3 level, but not GLUT1 level, was observed in the brain tissues of several scrapie experimental animals and scrapie-infected cell lines, Mol. Neurobiol. 49 (2) (2014) 991–1004.
[82] A. Vittori, C. Breda, M. Repici, M. Orth, R.A. Roos, T.F. Outeiro, et al., Copy-number variation of the neuronal glucose transporter gene SLC2A3 and age of onset in Huntington's disease, Hum. Mol. Genet. 23 (12) (2014) 3129–3137.